Mar. Freshwater Res., 2001, **52**, 937–963

A spatially disaggregated, length-based, age-structured population model of yellowfin tuna (*Thunnus albacares*) in the western and central Pacific Ocean

John Hampton[A] *and David A. Fournier*[B]

[A]Secretariat of the Pacific Community, BP D5, 98848 Noumea Cedex, New Caledonia. email: JohnH@spc.int
[B]Otter Research Ltd, PO Box 2040, Sidney, BC V8L 3S3, Canada

Abstract. A spatially disaggregated, length-based, age-structured model for yellowfin tuna (*Thunnus albacares*) in the western and central Pacific Ocean is described. Catch, effort, length-frequency and tagging data stratified by quarter (for the period 1962–99), seven model regions and 16 fisheries are used in the analysis. The model structure includes quarterly recruitment in each region, 20 quarterly age classes, independent growth patterns for juveniles and adults, structural time-series variation in catchability for all non-longline fisheries, age-specific natural mortality, and age-specific movement among the model regions. Acceptable fits to each component data set comprising the log-likelihood function were obtained. The model results suggest that declines in recruitment, and as a consequence, population biomass, have occurred in recent years. Although not obviously related to over-exploitation, the recruitment decline suggests that the productivity of the yellowfin tuna stock may currently be lower than it has been previously. Recent catch levels appear to have been maintained by increases in fishing mortality, possibly related to increased use of fish aggregation devices in the purse-seine fishery. A yield analysis indicates that average catches over the past three years may have slightly exceeded the maximum sustainable yield. The model results also reveal strong regional differences in the impact of fishing. Such heterogeneity in the fisheries and the impacts on them will need to be considered when future management measures are designed.

Additional keywords: length-based model, statistical age-structured model, spatial model, stock assessment

Introduction

Yellowfin tuna (*Thunnus albacares*) is an important component of the tuna fishery in the western and central Pacific Ocean (WCPO), with annual catches over the past decade averaging almost 400 000 t (Lawson 2000). Catches are distributed over a wide area, from the Philippines and Indonesia in the west to Hawaii, Kiribati and French Polynesia in the east (Fig. 1). The majority of the catch is taken by industrial purse seiners (~60%) and longliners (~17%), and by a variety of small-scale fishing gears (gill-net, troll, handline and others) in the Philippines and eastern Indonesia (~20%). Yellowfin tuna is believed to constitute a discrete genetic stock in the WCPO (Ward *et al.* 1994).

Previous assessments of yellowfin tuna in the WCPO have relied mainly on analyses of standardized longline catch-per-unit-effort (CPUE) and tagging data (Hampton *et al.* 1999). However, with formal international management arrangements for tuna fisheries in the WCPO currently being negotiated (Anon. 2000), there is a need for a more sophisticated assessment approach that can indicate the current status of the resource relative to defined biological reference points (Schnute and Richards 1998) and evaluate alternative harvest strategies. A model that sufficiently captures the complexity of the population dynamics and fisheries is required as a first step. In particular, because yellowfin tuna is captured at different ages by different gear types, such a model will need to incorporate age structure to be able to predict the stock response to changes in harvest levels by the different fisheries. Also, the wide distribution of the stock and fisheries coupled with spatial heterogeneity in yellowfin tuna fishery and population parameters (including movement patterns), requires treatment of the spatial distribution of the fisheries, the fish and fish movement.

The MULTIFAN-CL model (Fournier *et al.* 1998) provides a good basis for a spatially disaggregated, age-structured model for yellowfin tuna. MULTIFAN-CL is age structured, with the age composition of catches being estimated from length-frequency samples. The model is spatially disaggregated, with the population and fisheries stratified into a number of regions within the overall stock range. Other features of the model, such as the treatment of process error in the fishing effort – fishing mortality

 10.1071/MF01049 1323-1650/01/070937

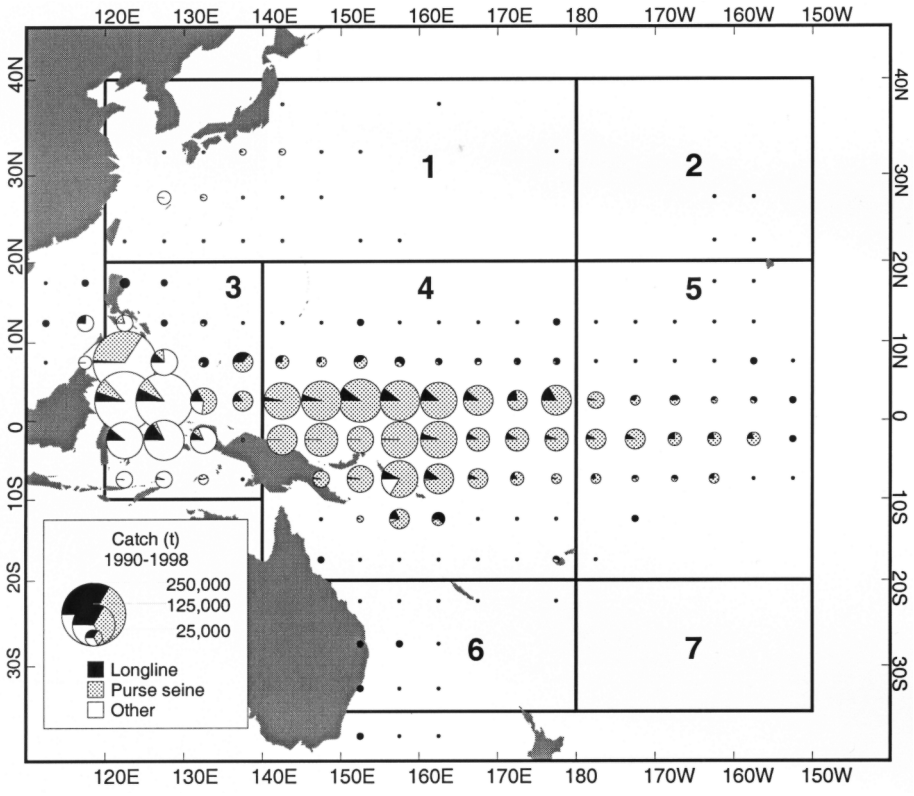

Fig. 1. Distribution of yellowfin tuna catch by gear type in the WCPO, 1990–98, and the seven-region spatial stratification used in the model.

relationship, also make it a suitable choice as a starting point for a yellowfin tuna stock assessment model.

This paper describes the adaptation and extension of the MULTIFAN-CL model for the stock assessment of yellowfin tuna in the WCPO. The major extension of the model involves the incorporation of tagging data into the model to facilitate the estimation of age-dependent movement and natural mortality rates. Various adaptations of the model to deal with specific features of yellowfin tuna biology (e.g. non-von Bertalanffy growth of juveniles) and fisheries are described as a base-case example. A yield analysis is integrated into the model as an example of how the model results might be interpreted in a fishery management context.

Methods

Below, we describe the conceptual basis of the population dynamics model, the data used in the model and the parameter estimation procedures employed. The full mathematical specification of the model and the various components of the likelihood function are given in a series of appendices.

Population dynamics model

The equations specifying the population dynamics of yellowfin tuna are given in Appendix A. The model is age-structured, with twenty quarterly age-classes considered (Eqns A.1–A.2). The final age-class is an aggregate of all fish of that age and older. The time intervals in the model are quarters (Jan–Mar, Apr–Jun, Jul–Sep, Oct–Dec), and the time period covered by the analysis extends from 1962 to 1999. Spatial structure is incorporated by modelling the yellowfin tuna population separately in seven regions (Fig. 1). These regions reflect the distribution of the various fisheries defined in the model and the spatial resolution of some of the data.

Recruitment of yellowfin tuna is assumed to occur at the beginning of each quarter. Earlier attempts to fit an annual recruitment model proved unsuccessful because of the lack of an annual recruitment signal in the majority of the length-frequency data. This was not unexpected, because yellowfin tuna spawning does not follow a clear annual pattern in the tropics, but seems to occur sporadically when food supplies are plentiful (Itano 2000). Recruitment is parameterized as the product of a spatially aggregated average recruitment, a vector specifying the time-series variation (lognormally distributed) in spatially aggregated recruitment, a vector specifying the average distribution of recruitment among the regions and a matrix specifying the time-series variation in the spatial distribution of recruitment (Eqn A.1). Spatially aggregated recruitment may be assumed to have a weak association with spawning biomass via a Beverton and Holt stock–recruitment relationship. This assumption is optional, but is required if the model results are to be used in a yield analysis. The assumption is introduced by means of a small penalty on the objective function (see Appendix D, Eqns D.6 and D.7).

The age structures of the region-specific initial populations are assumed to be at equilibria defined by the average total mortalities in each region over the initial 20 quarters (Eqn A.3). Catches were relatively low (~50 000 t per year) during this period and similar to those in the years immediately preceding 1962.

Movement of yellowfin tuna among the regions is assumed to occur instantaneously at the beginning of each quarter (Eqns A.4, A.5). Movement is age-dependent (Eqn A.6) and is assumed to be time-

Table 1. The definition of fisheries used in the model
The spatial configuration of the model regions is shown in Fig. 1

Fishery	Model region	Gear type/fishing method
PR	3	Philippines ringnet/purse seine
PH	3	Philippines handline
IN	3	Indonesia various
PA3	3	Purse-seine associated sets
PU3	3	Purse-seine unassociated sets
PA4	4	Purse-seine associated sets
PU4	4	Purse-seine unassociated sets
PA5	5	Purse-seine associated sets
PU5	5	Purse-seine unassociated sets
L1	1	Longline
L2	2	Longline
L3	3	Longline
L4	4	Longline
L5	5	Longline
L6	6	Longline
L7	7	Longline

invariant. We are therefore attempting to capture only the general pattern of cohort dispersal over time, and not model the detailed movement dynamics of yellowfin tuna, which are likely to be highly variable and affected by a range of biological and physical factors. Natural mortality is assumed to be age-dependent, but time- and region-invariant.

Sixteen fisheries are defined on the basis of gear type, set type in the case of purse-seine gear, and region of operation (Table 1). Catch and fishing mortality are fishery-, age- and time-specific (Eqn A.7), with fishing mortality partitioned into age-dependent (selectivity) and time-dependent components (catchability and effort) (Doubleday 1976; Paloheimo 1980; Fournier and Archibald 1982; Fournier *et al.* 1998). A process error term (effort deviations) was included in the effort–fishing mortality relationship (Eqn A.8) to acknowledge the stochastic variability that occurs in most fisheries.

Selectivity is fishery-specific and assumed to be time-invariant. Selectivity coefficients have a range of 0–1, and for the longline fisheries (which catch almost exclusively adult yellowfin tuna) are assumed to increase monotonically with age. The coefficients are expressed as age-specific parameters, but are smoothed according to the degree of length overlap between adjacent age classes (Eqns A.9–A.12). This is appropriate where selectivity is thought to be a fundamentally length-based process (Fournier *et al.* 1998). The coefficients for the last four age classes are constrained to be equal, because the mean lengths for these age classes are very similar. All longline fisheries except L1 are assumed to have common selectivity coefficients. Selectivity coefficients for L1 are estimated separately because preliminary analyses using a model incorporating common selectivity for all longline fisheries resulted in a poor fit to the L1 length-frequency data.

Catchability is allowed to vary slowly over time (akin to a random walk) for the non-longline fisheries using a structural time-series approach (Gudmundsson 1994) (Eqn A.13) with 'random-walk' steps taken every three years. Catchability for the longline fisheries is assumed to be constant over time and among regions (the rationale for this is explained in the next section). Seasonal variability in catchability is allowed for all fisheries for which quarterly data were available (all except the PR, PH and IN fisheries) (Eqn A.14).

Length-frequency data were used to estimate catch age composition, and therefore some assumptions need to be made concerning the length distribution of the fish (Fournier *et al.* 1990). These assumptions are *(i)* that lengths of the fish in each age-class are normally distributed (Eqns A.15–A.17) *(ii)* that mean lengths-at-age of age-classes 9 through 20 lie on a von Bertalanffy growth curve (Eqn A.18) and *(iii)* that standard deviations of the lengths for each age-class are a linear function of the mean length-at-age (Eqn A.19). Regarding assumption (ii), previous analyses (Lehodey and Leroy 1998) revealed significant departure from von Bertalanffy growth of juvenile yellowfin, so the mean lengths of the first 8 age-classes were allowed to be independent parameters of the model.

The spawning biomass of the population is a quantity that is often monitored for management purposes. We use spawning biomass to estimate the stock–recruitment relationship for the yield analysis and compute it as a function of numbers-at-age, the proportion of mature fish in each age-class and the average weight of fish in each age-class (Eqns A.20, A.21).

Dynamics of tagged yellowfin tuna

Several modifications of this general population dynamics model for yellowfin tuna are required to model the dynamics of the tagged fish (Appendix B). The main difference is that the tagged population is stratified by 'cohorts' (releases in a particular region during a particular time period) and recruitment to the tagged population occurs when tagged cohorts are released (Eqns B.1, B.2).

Tag recaptures are predicted in an equation similar to that for the general population (Eqn B.3). Because not all tag recaptures were reported, fishery-specific tag-reporting rates are incorporated into Eqn B.3.

For the tagged population and the general population to share fishing mortality parameters, it must be assumed that the tagged fish become randomly mixed with the general population within the spatial strata being considered. As the regions defined in the yellowfin tuna model are large, it is likely that this assumption will not be satisfied soon after release. The approach that we have taken is to define a number (one, in this case) of initial time periods after release as 'pre-mixed' periods and to compute fishing mortality rates for each tag-release cohort during such periods based on the observed recaptures and estimated tag-reporting rates. This or similar procedures are commonly applied in analyses of tagging data (e.g. Hoenig *et al.* 1998, Bertignac *et al.* 1999, Hampton 2000).

Data used in the model

The model parameters are estimated by minimizing an objective function that comprises the sum of the negative log-likelihoods of the data and various penalties that constrain the parameterization. The data component of the objective function comprises the log-likelihoods of the observed total (i.e. age-aggregated) catches by time period and fishery, the observed length-frequency proportions by time period and fishery and the observed tag recaptures by tag-release cohort, age-class, time period and fishery. The form of the log-likelihood function for each of these data categories is detailed in Appendix C. Below we describe the important aspects of the structure and variability of each data set. Effort data are not 'data' in the sense that they are predicted and used to fit the model, but may be thought of as priors for effective effort. The effort data are also included in the data description given below.

The catch data (Fig. 2) define the occurrence of a fishery in a particular time period, termed a fishing incident. The yellowfin tuna data comprise 1941 fishing incidents across the 16 fisheries and 152 quarterly time periods covered by the analysis. Data for the longline fisheries for 1999 were not available at the time of analysis, and were assumed to be the same as for the corresponding quarters in 1998.

The catch data are modelled by using the sum of squared residuals in the log of the observed and predicted catches (Eqn C.1), which may be expressed in either numbers or weight of fish for each fishing incident in a particular fishery. Catches are expressed in numbers of

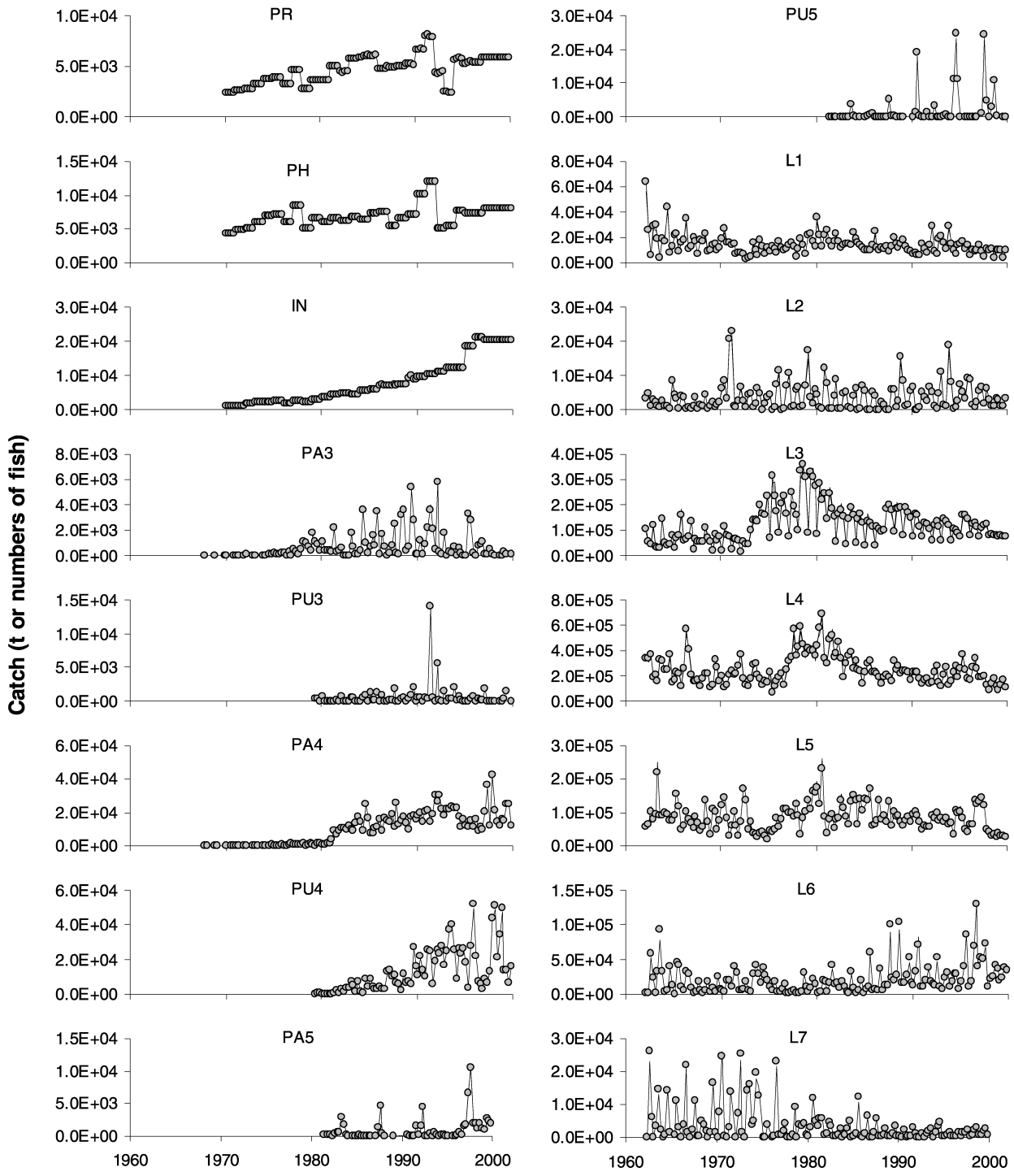

Fig. 2. Time series of observed (circles) and predicted (lines) catches by fishery. The fishery codes are defined in Table 1. Catches are in number of fish for fisheries L1-L7 and in tonnes for all other fisheries.

fish for the longline fisheries and in weight for the other fisheries, consistent with logbook and other catch recording methods used in the fisheries. We assume that the total catch data are observed with no bias and relatively high precision (equivalent to a residual s.d. of 0.07).

Effort data were available for all fishing incidents for all fisheries other than the PR, PH and IN fisheries, for which no effort data were available, and for 1999 for the longline fisheries. In these cases, effort data were defined as 'missing', a nominal value of effort was assumed and the effort deviations were given sufficient flexibility to allow the catch to be accurately predicted.

Effort for purse-seine fisheries is measured as days fishing and/or searching, and is allocated to either associated sets (sets on floating

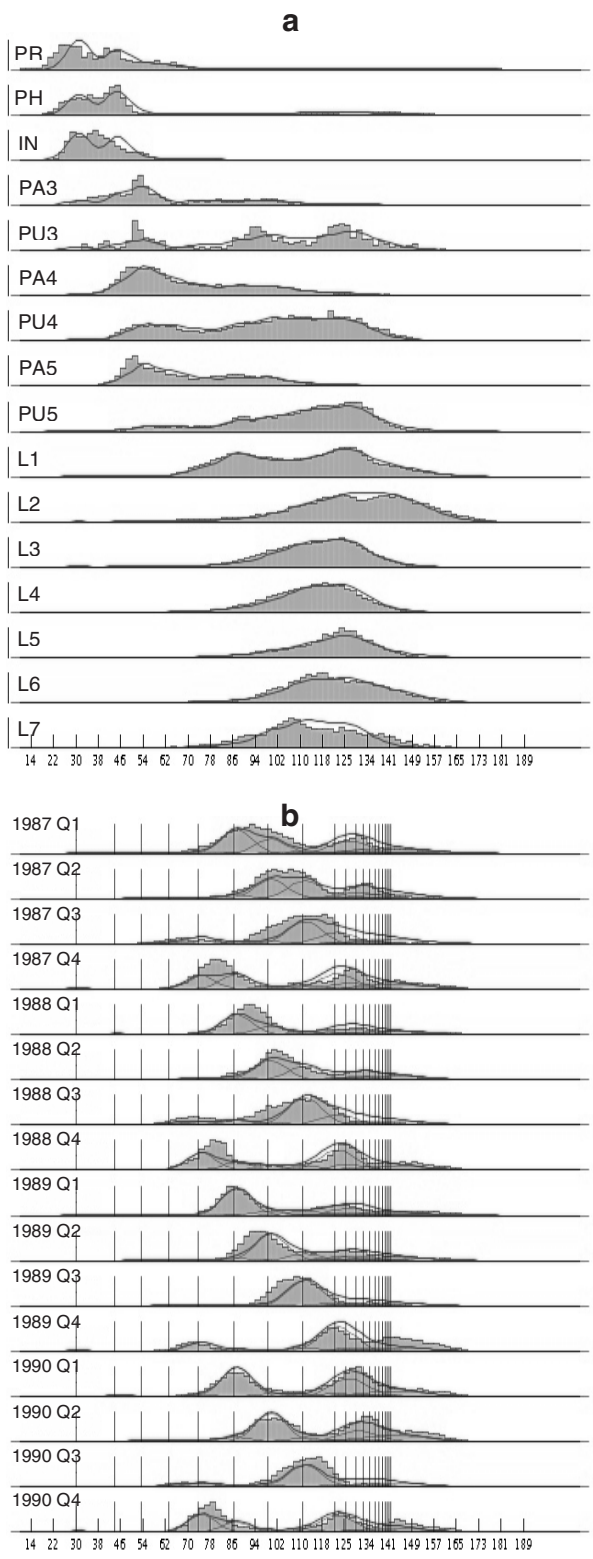

Fig. 3. Observed (histograms) and predicted (lines) length-frequency data for *(a)* each fishery aggregated over time and *(b)* for fishery L1 in 16 successive quarters from 1987 to 1990. The fishery codes in (a) are defined in Table 1. The vertical lines in (b) mark the estimated mean lengths for each age class in each period.

objects such as logs and fish aggregation devices (FADs)) or unassociated sets (sets on free-swimming tuna schools) based on the proportion of total sets attributed to those set types in logbook data. For the longline fisheries, we used estimates of standardized effort derived in a separate study (Bigelow *et al.* 1999). Essentially, standardized effort is an estimate of the numbers of longline hooks fishing in the mixed layer above the thermocline, which is believed to define yellowfin tuna habitat. The estimates take into account the time and spatial variability in the depth of the mixed layer (using oceanographic databases) and variation in the fishing depth of longliners as indicated by distributions of the numbers of hooks between floats. The standardized effort estimates were derived at 5°-month resolution separately for the Japanese, Korean and Taiwanese distant-water longline fleets. The estimates were then summed across these fleets and aggregated into the spatial and temporal stratification used in the model. Longline effort in each fishery was divided by the relative size of the respective region, allowing longline CPUE to index abundance in each region (rather than density). This allowed simplifying assumptions to be made regarding the spatial and temporal stability of catchability for the longline fisheries.

Length-frequency data (Fig. 3) were available for only a limited period in the 1990s for the PR, PH and IN fisheries, and after 1984 for the purse-seine fisheries. Length-frequency data were available for each of the longline fisheries over the entire period of the analysis. It was assumed that individual length-frequency samples (taken at a particular vessel unloading by port samplers, or on a particular day by observers) represented random samples of the catch length composition for that fishery and time period. Such individual length-frequency samples were therefore simply aggregated without weighting to produce the data by fishery and time period. The length-frequency proportions are modelled by use of a robust normal likelihood function (Eqns C.4–C.6). For computing the variance, the maximum length-frequency sample size is limited to 1000 and the variance expanded by a factor of 10 to acknowledge non-random sampling.

Yellowfin tuna tagging data (Kaltongga 1998: Fig. 4) were aggregated in a similar fashion to the fishery data. Tag releases from 1989 to 1992 were aggregated into 25 release cohorts (by quarter and region). The age structure of release cohorts is estimated internally by the model, as described earlier. Recaptures are classified by age-class, quarter and recapture fishery. The age-class at recapture is obtained by adding the number of time periods between release and recapture to the estimated age-class at release. The two purse-seine fisheries in each of regions 3, 4 and 5 were grouped for the purposes of modelling tag returns because information on set type (associated or unassociated sets) was not consistently provided with tag returns. Overall, 39424 releases and 4231 tag returns were included in the analysis. The tag-return data are modelled using a log negative binomial likelihood function (Eqn C.11), which explicitly acknowledges overdispersion of the tagging data relative to Poisson or multinomial probabilities.

Penalties on the objective function

The base-case model has a total of 3396 estimated parameters, including process error variables. Extensive use is made of penalties on the objective function to constrain the parameterization of the model. These penalties may be thought of as incorporating prior information into the model. For example, prior distributions on the effort deviations ε_{t,f_r} (Eqn A.9) and the catchability deviations η_{y,f_r} (Eqn A.14) are used to constrain the variability of these process error terms. The various penalty functions are described in Appendix D. A complete listing of estimated parameters, and a brief description of their constraints, is given in Appendix E.

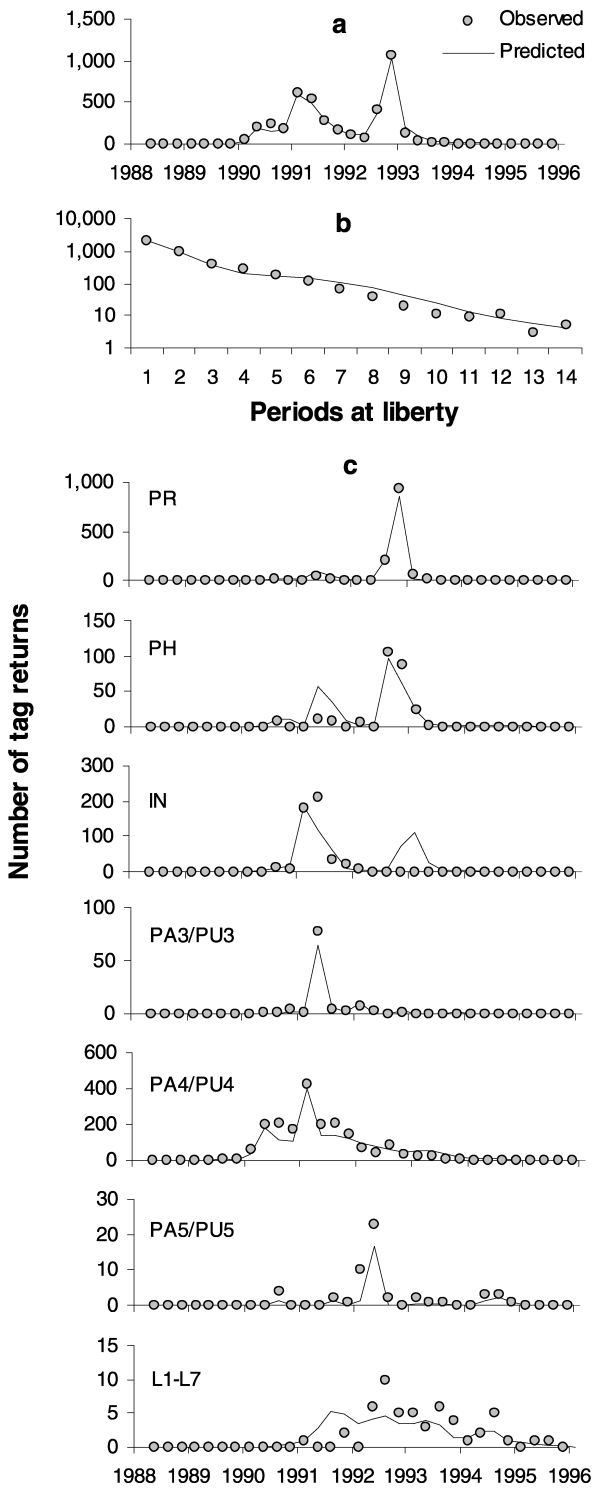

Fig. 4. Observed and predicted tag returns by *(a)* time period, *(b)* time at liberty, and *(c)* time period and fishery grouping (see Table 1 for definition of fishery codes).

Parameter estimation

The parameters of the model are estimated by minimizing the sum of the data contributions to the objective function (C.1, C.4, C.11) and the contributions of the penalties (D.1, D.3–D.5, D.7–D.12). The minimization is performed by an efficient optimization using exact derivatives with respect to the model parameters. The derivatives are calculated by an extension of automatic differentiation (Griewank and Corliss 1991) implemented in the AUTODIF C++ library (Otter Research Ltd 1994). The method also provides estimates of the Hessian matrix at the mode of the posterior distribution (see Fournier *et al.* 1998 for details), which we use in conjunction with the delta method (Seber 1973) to obtain estimates of the covariance matrix and approximate confidence intervals for the model parameters and derived quantities of interest.

The model was fitted to the data from arbitrary starting conditions by a phased estimation procedure. The initial phase employed a relatively simple model structure (age-independent and fixed natural mortality and movement, constant catchability for all fisheries, fixed distribution of recruitment among regions, fixed Brody growth coefficient and other simplifying assumptions). For subsequent phases, the model's assumptions were progressively relaxed and additional parameters estimated. In the final phase, all parameters for the base-case model were estimated simultaneously.

Results and discussion

Fit of the model to the data

The fit of the model to the total catch data by fishery is very good (Fig. 2), reflecting our assumption that observation errors in the total catch estimates are relatively small.

The fit to the length data is displayed in Fig. 3*a* for length samples aggregated over time for each fishery. Note that this is not the form in which the data enter the model, but is a convenient way of assessing the overall fit of the model to the length data for each fishery. On the whole, the model appears to have captured the main features of the data, particularly for the larger, more heavily sampled fisheries. The modal structure evident in the PR, PH, IN fisheries and in some of the purse-seine fisheries is well represented by the model predictions, while the shape and location of the length distributions of all fisheries is well estimated.

There is more variability in the fits when the data are disaggregated by time period, but on the whole the modal structure of the various samples and modal progression over time seem to be consistently interpreted by the model. A good example of modal progression and seasonal recruitment to the fishery can be seen in fishery L1 (Fig. 3*b*). The modal structure and progression are very clear in these samples and the model has replicated these features very well.

The fit of the model to the tagging data compiled in various ways is shown in Fig. 4. The fit to the total tagging data by calendar time period (Fig. 4*a*) and by time at liberty (Fig. 4*b*) are both satisfactory. For the data classified by fishery (Fig. 4*c*), the fits are mostly satisfactory for the fisheries returning large numbers of tags. The exception to this is the IN fishery, where ~200 tag returns were predicted by the model to have occurred in late 1992 and early 1993, but almost none was observed. The predicted returns are largely the result of tag releases made in the Philippines during late 1992. The tags used in this component of the

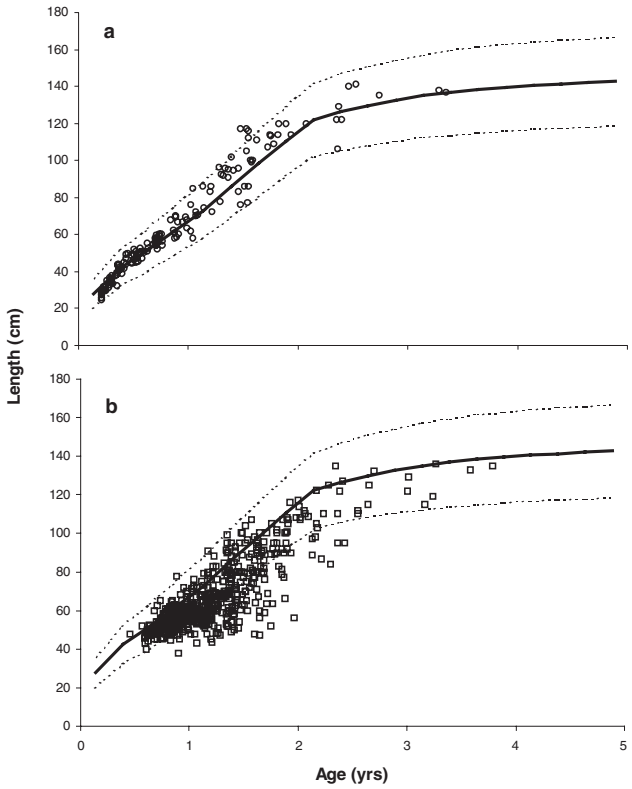

Fig. 5. Estimated yellowfin tuna growth curve (dark line) ± 2 s.d. in length-at-age (dotted lines). Ages on the *x*-axis assume that the age of the first age-class is ~0.2 year. *(a)* Length-at-age observations based on daily ring counts from otoliths. *(b)* Length-at-age estimates for recaptured tagged yellowfin tuna (age-at-recapture determined by estimating age-at-release from length-at-release using a growth curve based on the otolith data, and adding time at liberty); only tag returns at liberty for more than 100 days are shown.

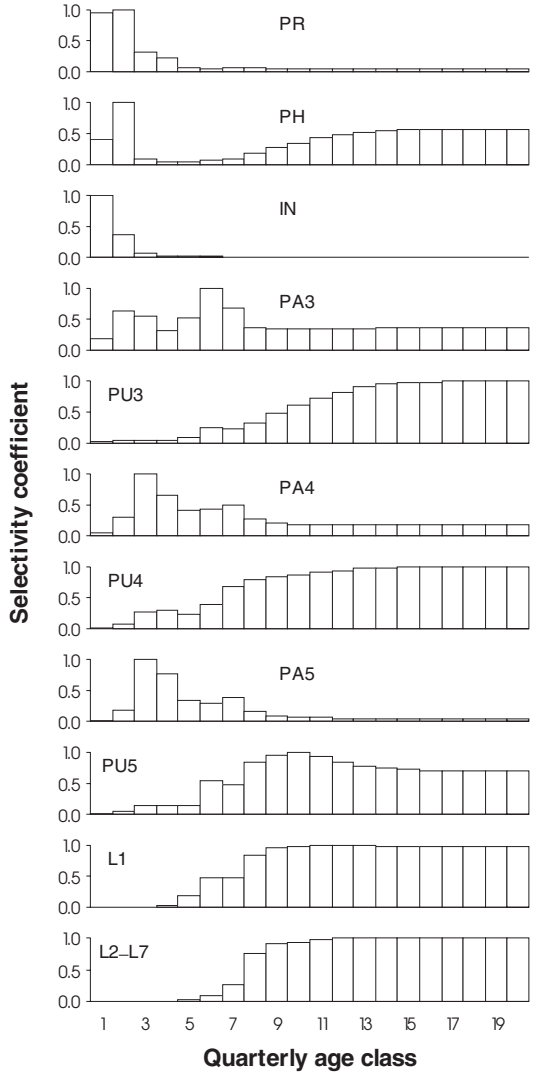

Fig. 6. Estimated selectivity coefficients, by fishery (see Table 1 for definition of fishery codes).

tagging project were identifiably of Philippines origin, and differentially high non-reporting of recaptures of these tags by Indonesian fishermen is suspected to have occurred. This might explain the discrepancy between observed and predicted returns in the IN fishery at this time.

Growth estimates

Using the four-cohort-per-year formulation, the model was able to detect a coherent growth signal in the size data. The non-von Bertalanffy growth of juvenile yellowfin is evident, with a pronounced reduction in growth rate in the 40–70 cm size range (Fig. 5). This growth pattern and the estimated growth curve in general are corroborated by estimates of length-at-age obtained from reading daily increments on yellowfin tuna otoliths (Lehodey and Leroy 1998) (Fig. 5*a*). Estimates of length-at-age for yellowfin tuna tag returns at the time of recapture (Secretariat of the Pacific Community, unpublished) can also be derived, assuming that age at release is well estimated by an age–length relationship based on the otolith data. These estimates are more variable than the otolith data, but evidence of the reduction in growth rate in the 40–70 cm size range is also present (Fig. 5*b*). However, the lengths at recapture are on average somewhat smaller than would be predicted by either the otolith data or the estimates obtained from this model. The reason for this inconsistency is not known. A negative effect of tagging on growth has been observed in other tunas (e.g. Hampton 1986) and this could also be the case for yellowfin tuna.

Selectivity estimates

Selectivity coefficients for each fishery (Fig. 6) are assumed to be stable over time. Note that the variability of the coefficients is constrained to some extent by smoothing penalties, the coefficients for the longline fisheries are assumed to increase with age and the coefficients for fisheries L2–L7 are assumed to be common.

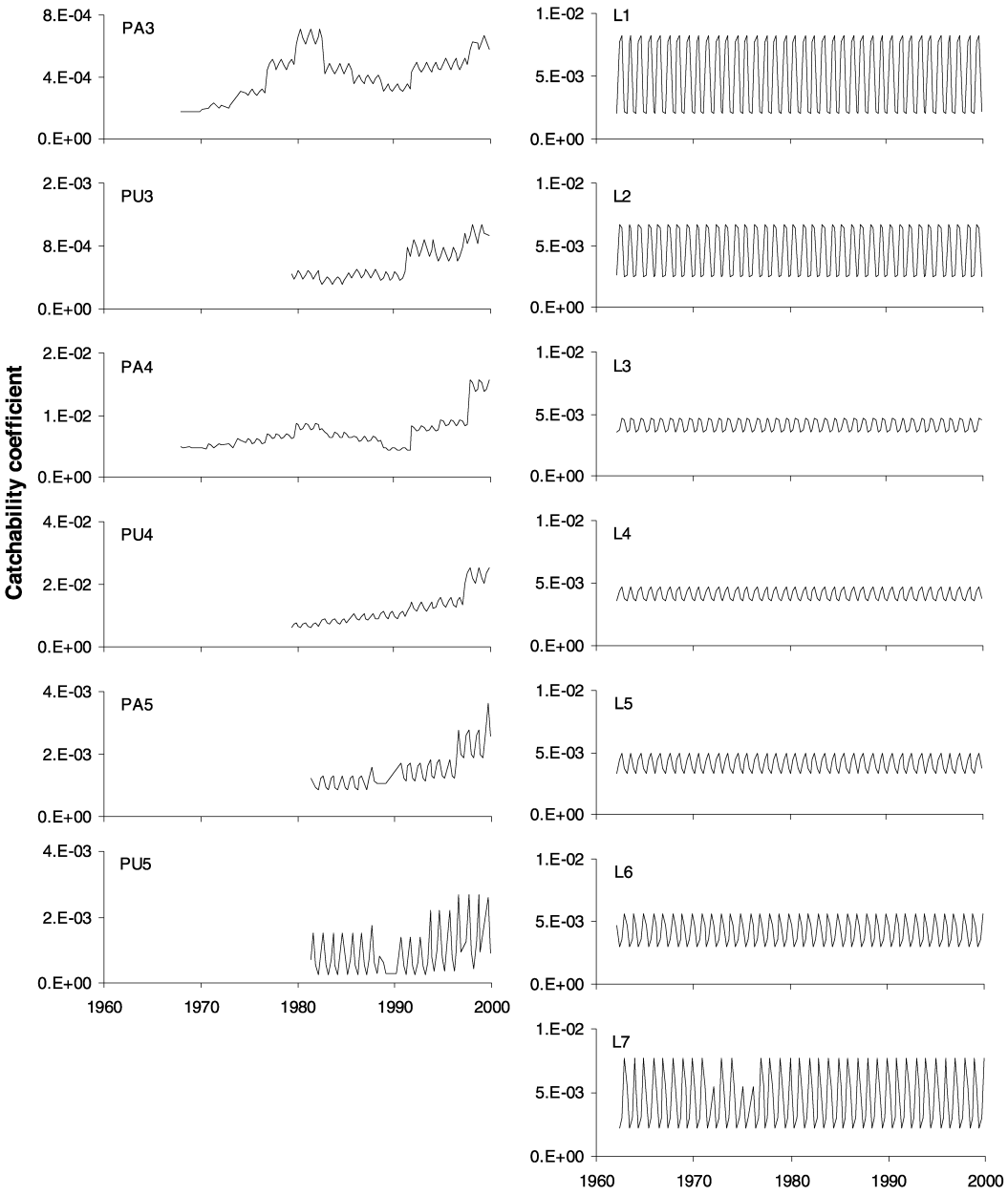

Fig. 7. Estimated time series of catchability, by fishery (see Table 1 for definition of fishery codes).

Catchability estimates

Time-series changes in catchability are evident for several fisheries (Fig. 7). There is evidence of strongly increasing catchability in the PA4 fishery in the late 1990s. During this period, the use of drifting FADs increased dramatically. The locations of FADs are monitored electronically by the deploying vessels, and in some cases the FADs are equipped with echo sounders to detect the presence of tuna. It is likely that these developments have increased the operational efficiency of purse-seine vessels, which may explain the increased catchability towards the end of the time series. Increases in catchability are also estimated for some of the other purse-seine fisheries, e.g. the PU4 and PA5 fisheries.

Seasonal variation in catchability is apparent in all longline fisheries, but is greater for the L1 and L2 fisheries (northern temperate), and the L6 and L7 fisheries (southern temperate). The phases of the seasonality in the north and south are offset by ~0.5 years, as expected (Fig. 8).

The overall consistency of the model with the observed effort data can be examined in plots of effort deviations (Fig. 9) against time for each fishery. If the model is coherent with the effort data, we would expect an even scatter of effort deviations about zero. Some outliers would

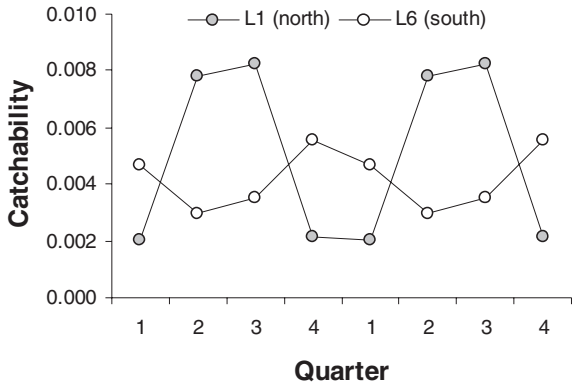

Fig. 8. Seasonal patterns in catchability for longline fisheries in northern (L1) and southern (L6) regions of the model area.

also be expected, which prompted the use of robust estimation techniques. On the other hand, if there was an obvious trend in the effort deviations with time, this may indicate that a trend in catchability had occurred and that this had not been sufficiently captured by the model. No unusual variability in the residuals is apparent in Fig. 9, suggesting that the model has extracted all the information present in the data regarding catchability variation.

Fig. 9 also provides an indication of the relative variability of the effort data with respect to the model. The plots suggest that the data for the L3, L4 and L5 fisheries (the longline fisheries in the tropics) provide the best information on the stock dynamics.

For the longline fisheries, we assumed catchability to be constant among regions, as well as over time (with the exception of seasonal variation). This assumption was considered appropriate because of the use of standardized effort for these fisheries, i.e. the numbers of longline hooks fishing in yellowfin tuna habitat (the upper mixed layer) in a standardized area. Given this assumption and treatment of the longline effort data, we would expect that longline CPUE would provide an index of exploitable abundance (population-at-age multiplied by age-specific selectivity and summed across age-classes) in each region. The time-averaged relative levels of exploitable abundance and CPUE among regions are almost identical (Fig. 10), which is consistent with the assumption of constant longline catchability among regions. Fig. 11 compares exploitable biomass and CPUE for each region individually. There is generally good agreement between the time-series patterns of the two variables in each region. This indicates that the model has incorporated the information on longline CPUE into the stock dynamics as intended by the catchability assumptions.

Natural mortality rate estimates

The estimated natural mortality rates are allowed to vary with age class (Fig. 12). For the mid-sizes of ~55–90 cm, the estimates are in the range 0.6–0.7 year^{-1}, which is consistent with values commonly assumed for yellowfin tuna in other areas. The right-hand end of the curve begins its upward movement at around the size at first maturity. After ~130 cm in size, M is estimated to decline sharply. One possible interpretation of this pattern is that the high energetic requirements of spawning in female yellowfin tuna (Schaefer 1996) cause higher female mortality, with aggregate M falling at larger size as females make up a declining proportion of the population. The declining incidence of yellowfin tuna females with increasing fish size (Schaefer 1998; Secretariat of the Pacific Community, unpublished) is congruent with this explanation. Such size-related changes in natural mortality and sex ratio have been estimated in other tunas as well (Fournier *et al.* 1998; Hampton 2000). If the hypothesis regarding mortality-related changes in sex ratio is correct, then the addition of sex-ratio data as a component of the objective function may provide useful information on age-specific natural mortality in tuna population dynamics models.

Movement rate estimates

A representation of the dispersal patterns resulting from the estimated movement parameters is shown in Fig. 13, which shows the changes in the relative distributions over time of cohorts originating in each region. Yellowfin tuna originating in regions 1 and 6 appear to have the strongest residence. Movement is probably better determined in the tropical regions (3, 4 and 5) because the majority of tag releases occurred there. Considerable exchange of fish from region 3 to region 4 and between regions 4 and 5 is evident.

It is also possible to use the movement coefficients, the average proportions of the total recruitment occurring in each region and the age-specific natural mortality rates to estimate the equilibrium stock composition (in either numbers or weight of fish) in each region in the absence of fishing (Fig. 14). The model results imply that 60% of the equilibrium biomass in region 1 would be composed of fish recruited in that region. The contributions of local recruitment to equilibrium biomass in the other regions is 50% (region 2), 60% (region 3), 70% (region 4), 15% (region 5), 60% (region 6) and 100% (region 7). An interesting outcome of organizing the model results in this way is that it might provide a means of incorporating stock composition data (e.g. from analysis of otolith micro-constituents) into the model to provide additional information on dispersal patterns.

Fishing mortality rate estimates and the impact of fishing on the stock

Annual age-specific fishing mortality rates for the stock as a whole are shown in Fig. 15. Fishing mortality for all ages has increased over time, with the highest levels being estimated for yellowfin tuna aged approximately 0–1 year. A large

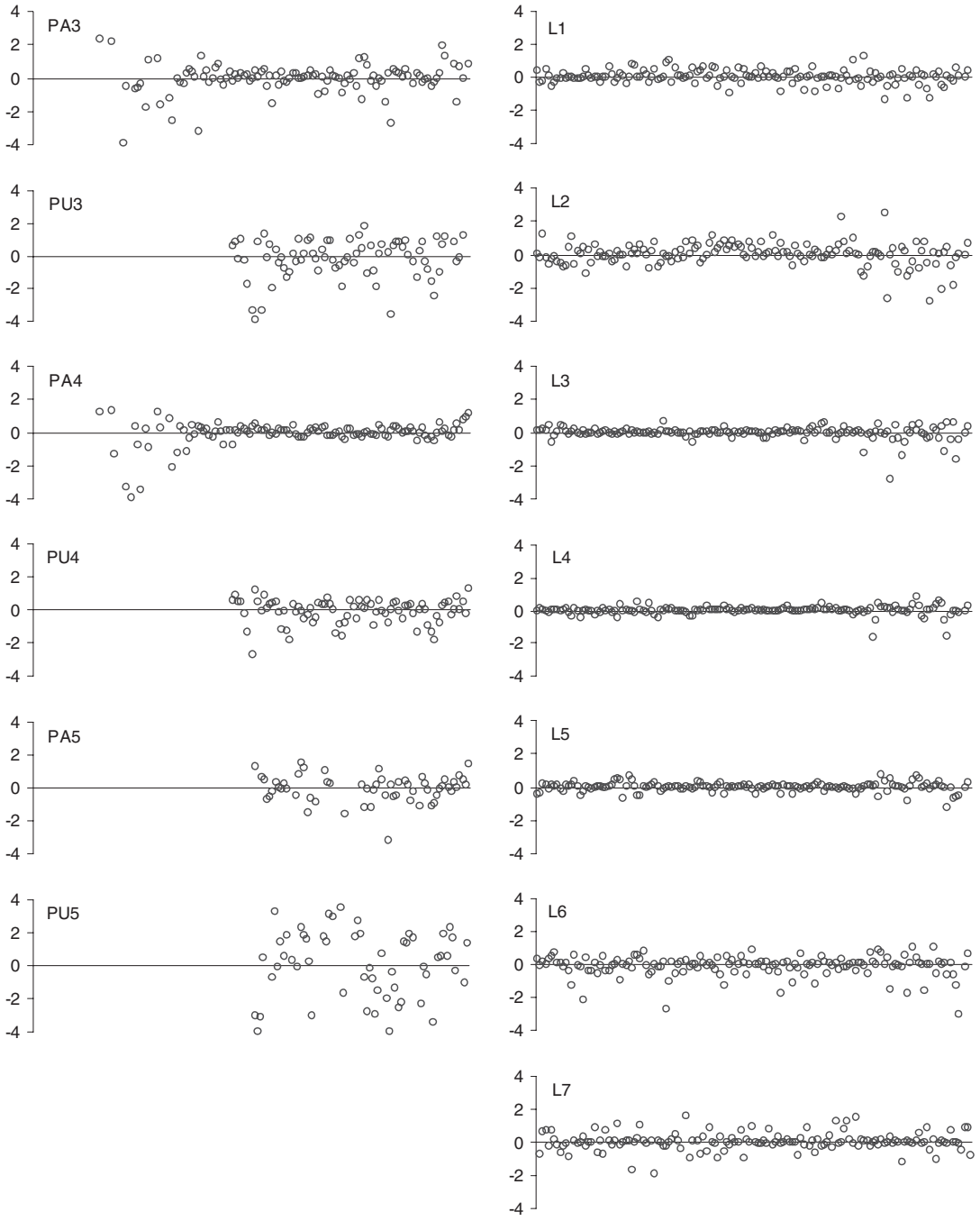

Fig. 9. Distributions of effort deviations over time, by fishery (see Table 1 for definition of fishery codes). The *x*-axis scale for each fishery is the same as in Fig. 7.

component of the exploitation of these small fish occurs in region 3 where they are targeted by the domestic fisheries of Philippines and Indonesia. For this age group, the fishing mortality rates in recent years exceed the corresponding age-specific natural mortality rate. For all other age groups the estimated fishing mortality rates are well below the corresponding natural mortality rates.

For a complex model such as this, it is difficult to readily interpret fishing mortality rates and other parameters to obtain a clear picture of the estimated impact of fishing on the stock. To facilitate this, we have computed total biomass trajectories for the population in each region using the estimated recruitment, natural mortality and movement parameters, but assuming that the fishing mortality was zero

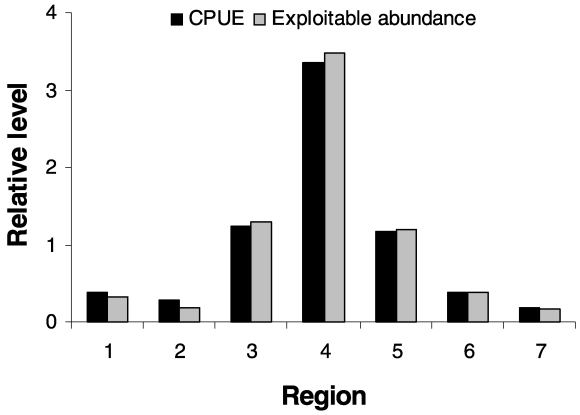

Fig. 10. 1962–99 average levels of longline CPUE and exploitable abundance in each region.

throughout the time series. Comparison of these biomass trajectories with those incorporating the actual levels of observed historical fishing provides a concise, integrated picture of the impacts of the total fishery on the stock. Biomass trajectories for each region and for the WCPO in total are shown in Fig. 16. There is very little difference between the 'actual' and the 'unfished' biomass trajectories in regions 1, 2, 6 and 7. The impact of fishing on the sub-populations in these regions can therefore be considered to be negligible. For regions 4 and 5, the difference between the 'actual' and 'unfished' trajectories is more significant. In region 4, the 'actual' biomass is ~44% below the 'unfished' biomass in 1999. For region 5, the difference is 26%. For region 3, there is much greater divergence between the two trajectories – in 1999, the 'actual' biomass is ~85% below the 'unfished' biomass. This result would suggest that there has been a large depletion of the sub-population in this region, primarily by the domestic fisheries of the Philippines and Indonesia.

Tag-reporting rate and overdispersion estimates

Tag-reporting rates were estimated for all fisheries, with relatively informative priors provided for the purse-seine fisheries (Table D1) for which independent information on tag-reporting rates was available from tag-seeding experiments (Hampton 1997). The estimated reporting rates (Fig. 17) are in the range of 0.50–0.75 for most of the fisheries, with the exception of the L3 and L5 fisheries, for which the estimated rates are ~0.15.

There was strong evidence of overdispersion of the tag-return data relative to Poisson or multinomial probabilities for the PR, PH, IN and all purse-seine fisheries. For these fisheries, the estimates of the negative binomial parameter determining the variance (see Eqn C.8) were all <5, indicating significant overdispersion. For the longline fisheries (which returned relatively few tags), there was no evidence of overdispersion.

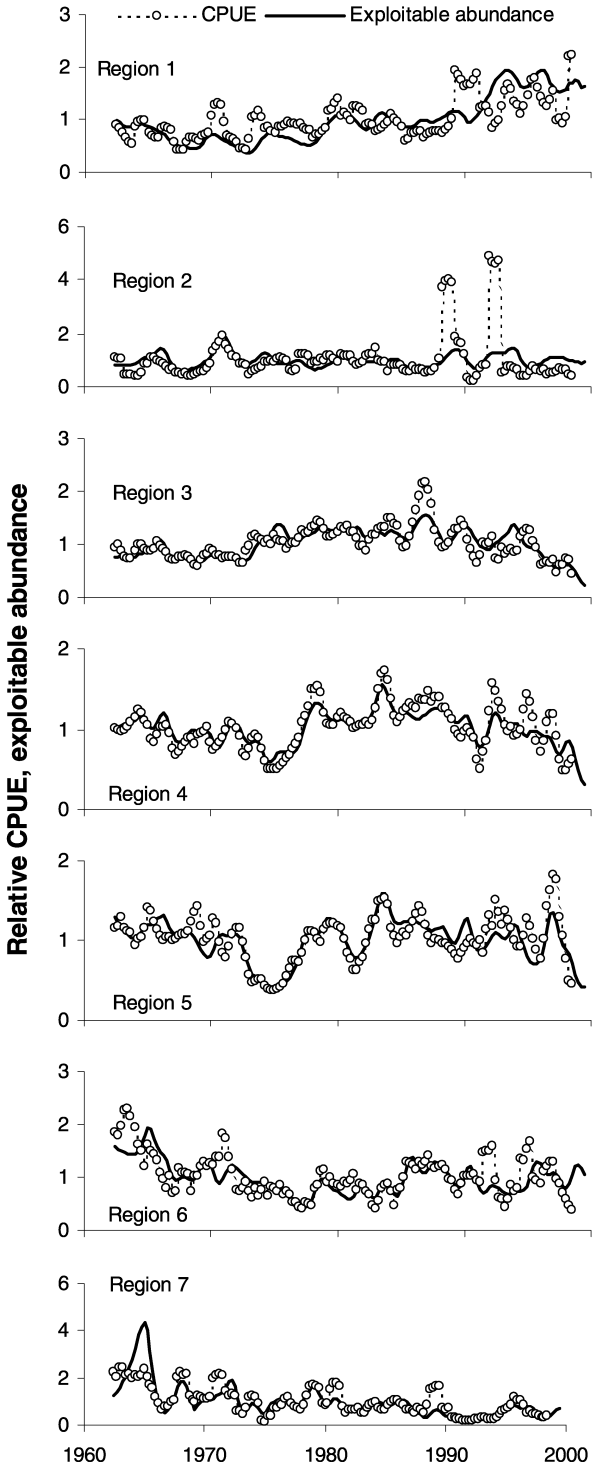

Fig. 11. Estimates of exploitable abundance and CPUE for the longline fisheries in each region. Both variables have been smoothed to remove seasonal variation.

Recruitment estimates

The recruitment estimates display considerable low- and high-frequency variation (Fig. 18). The low-frequency

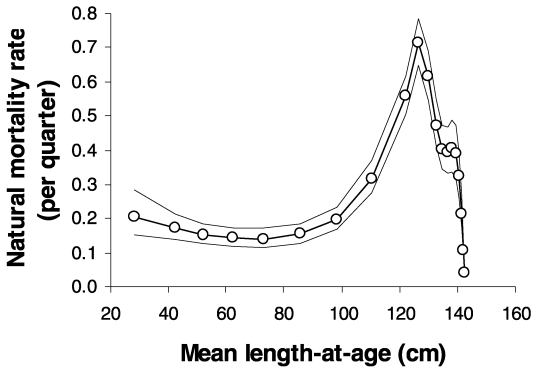

Fig. 12. Estimates of natural mortality rates by age class (circles) and 95% confidence intervals plotted against mean length.

variation might be correlated with decadal-scale environmental variation and some of the higher frequency variation to the El Niño–La Niña cycle, although these hypotheses have not yet been examined in detail.

The precision of the total-recruitment estimates (Fig. 18*a*) is indicated by the approximate 95% confidence intervals. For the whole period considered by the model, the average recruitment CV is 0.13. However, the CV is higher towards the end of the time series and is 0.25 and 0.50 for the last two quarters, respectively. This degradation in performance of recruitment estimates is expected for cohorts that have experienced relatively little fishing.

The average distribution of recruitment among the regions is estimated to be 30% of the total recruitment contributed by region 3, 47% by region 4 and 11% by region 5, with the remaining 12% contributed by the subtropical regions. This estimated average distribution is consistent with general biological understanding of yellowfin tuna spawning and recruitment in the WCPO.

Biomass estimates

Time series of total and spawning biomass by region are shown in Fig. 19. Most of the total population biomass is estimated to occur in the tropical regions 3, 4 and 5. However, greater proportions of the spawning biomass are located in the sub-tropical regions to the north (regions 1 and 2) and south (region 6), reflecting the dispersal of cohorts as they age.

Total and spawning biomass peaked in the early 1980s and have been trending downwards since that time. Total biomass is currently about 40% of the level in the early 1960s. The decline in spawning biomass has not been as severe, but the recent decline in recruitment is yet to affect the adult component of the stock to any great extent. However, the model predicts that further declines in spawning biomass will occur in coming years as these recent recruitments move through the population.

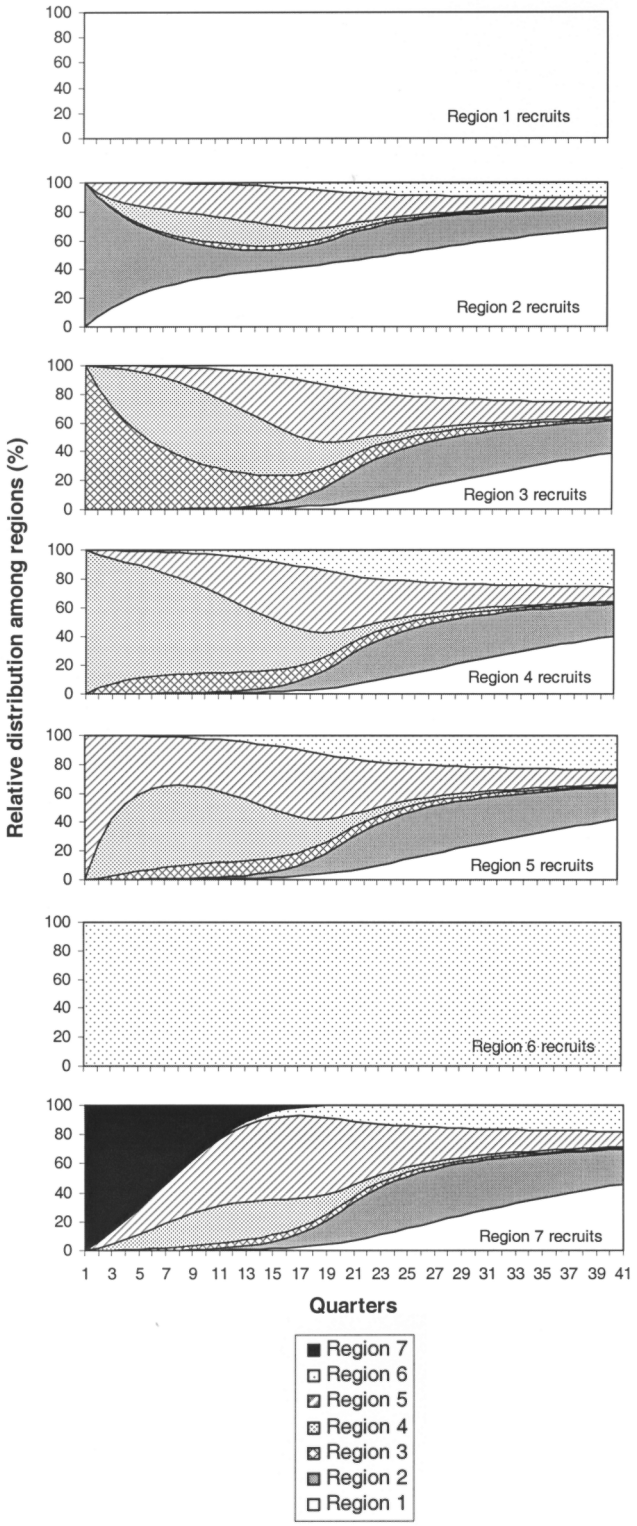

Fig. 13. Changes in the relative distributions among regions of cohorts originating in each region.

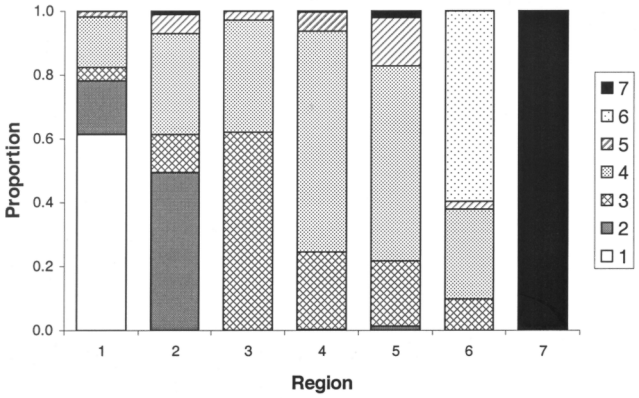

Fig. 14. Contribution of yellowfin tuna recruits from different regions (patterns within bars) to the stock biomass in each region (individual bars). Stock composition in each region was calculated in terms of biomass at equilibrium and in the absence of fishing.

Yield analysis and stock assessment

Many management agencies use reference points based on the concept of maximum sustainable yield (MSY). The concept was developed as part of the surplus production model, and has been commonly used in various forms over many years. However, surplus production models have many well-documented limitations, which has led to the development of more data-intensive and realistic population-dynamics models, such as the statistical age-structured model described in this paper.

Despite the widespread use of age-structured models in stock assessment, MSY remains enshrined as a management paradigm in international treaties and the fisheries legislation of many countries. Scientists are therefore often required to express the results of stock assessments in terms of MSY and related quantities, regardless of the type of population-dynamics model used. In the case of age-structured models, a yield analysis provides a convenient means of estimating MSY proxies. We have integrated a yield analysis into the overall parameter estimation, thus incorporating all parameter uncertainty into the results. The analysis comprises the following steps:

(*1*) Estimate a stock–recruitment relationship for predicting equilibrium recruitment from equilibrium spawning biomass.

(*2*) Specify the age-specific exploitation pattern to be used in the analysis; for yellowfin tuna, we have used the average WCPO fishing mortality rates for the last 12 quarters (i.e. 3 years) to define the age-specific exploitation pattern.

(*3*) Using the population dynamics model specified in Appendix A and the estimated stock–recruitment relationship, predict equilibrium yield for a series of fishing-effort multipliers.

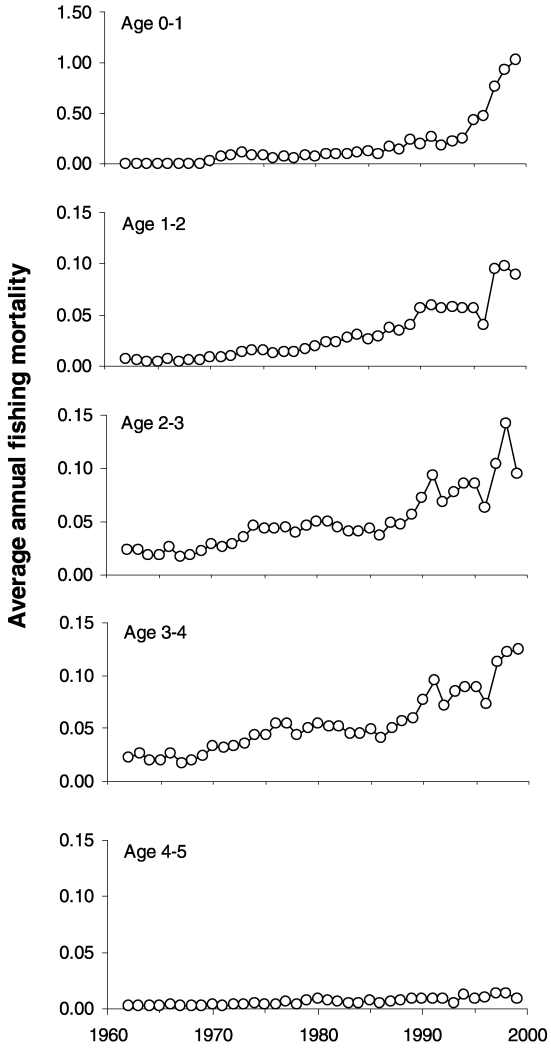

Fig. 15. Average annual fishing mortality rates by annual age groups for the entire model area.

In the estimated Beverton and Holt stock–recruitment relationship (Fig. 20), as is often the case with stock–recruitment estimates, there is a lot of noise and little apparent relationship with spawning biomass. Therefore, the estimated stock–recruitment relationship is very flat over most of the spawning biomass range, with significant decline in recruitment occurring only at spawning biomass levels below ~15% of the maximum spawning biomass. We cannot say with any certainty that this is really how recruitment would behave at low stock levels that have not yet been observed. This is an inherent problem with such analyses. Relative to the estimated recruitment variability, the 95% confidence intervals on the stock–recruitment curve seem unrealistically low. This is probably due to the inflexibility of the Beverton and Holt model.

The estimated equilibrium yield is plotted in Fig. 21. Yield is maximized at an effort multiplier of 1.1 (i.e. 10%

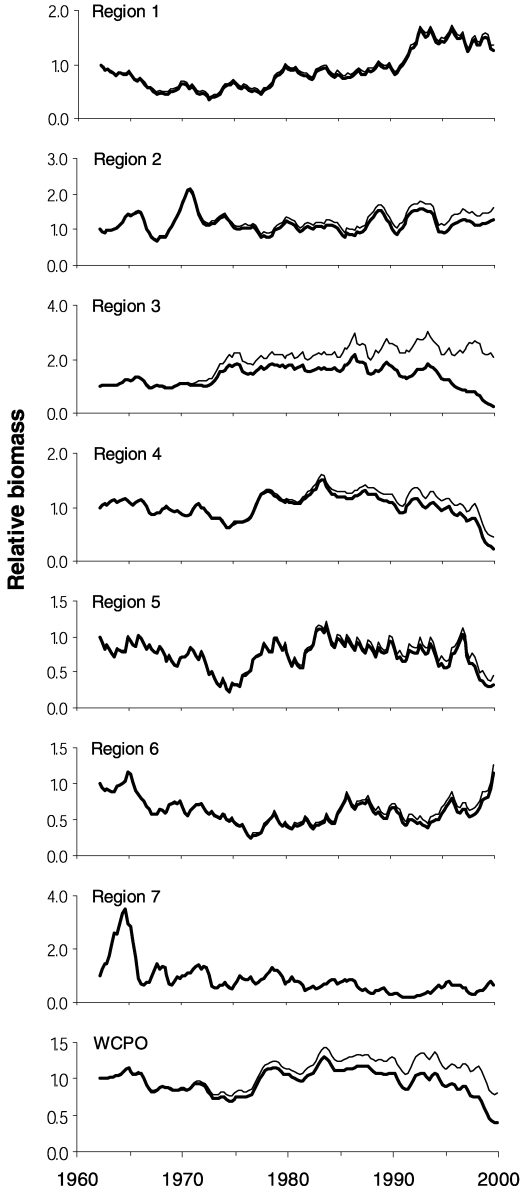

Fig. 16. Estimated biomass trajectories assuming the observed levels of fishing (heavy lines) and assuming no fishing (thin lines) for each region and for the WCPO. Trajectories plotted relative to estimated biomass in 1962.

higher than the 1997–99 average), and the MSY is ~85% (95% confidence intervals 71–98%) of the average 1997–99 catch, equivalent to ~367 000 (306 000–423 000) t. The yield-per-recruit curve follows an almost identical trajectory to the yield curve up to its maximum, but diverges at higher effort multipliers as effects on recruitment become significant. The 95% confidence intervals on the yield curve almost certainly underestimate the true uncertainty because they do not reflect the possibility of stock–recruitment model error.

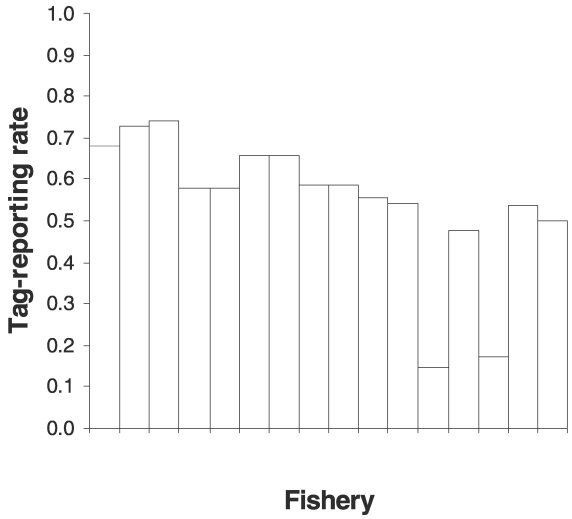

Fig. 17. Estimated tag-reporting rates for each fishery (see Table 1 for definition of fishery codes).

Conclusions

The length-based age-structured model that we have developed for yellowfin tuna in the WCPO is considerably more complex than those typically used in fisheries applications. As a consequence, the model is data intensive, but it allows considerable flexibility in modelling complex biological and fisheries processes, many of which have direct implications for international management of yellowfin tuna and other highly migratory species in the WCPO. For example, the combination of age and spatial structure in the model has allowed us to capture important heterogeneity in population distribution and exploitation. Such information will be critical for the management of highly migratory fish stocks in a multi-national, multi-gear fishery. Also, the estimation of time-series trends in catchability recognizes the reality that units of fishing effort are rarely static over long periods of time in fisheries – the effectiveness of fishing effort is liable to change because of environmental and technological change in particular. When, as is often the case, such changes cannot be directly incorporated into estimates of fishing effort, the structural time-series approach to catchability variation employed here is a useful modelling alternative.

Of course, the complexity that results from modelling these and other processes does not come without a cost. A single, phased estimation for the yellowfin tuna model takes of the order of 12 h on a high-end desktop computer, and a similar amount of time to compute the covariance matrix. This limits our ability to test a large number of alternatives to the base-case model structure. It also precludes, at this stage, a pure Bayesian treatment of parameter uncertainty and statistical inference (which would be preferable to the use of the Hessian matrix-delta method) through numerical

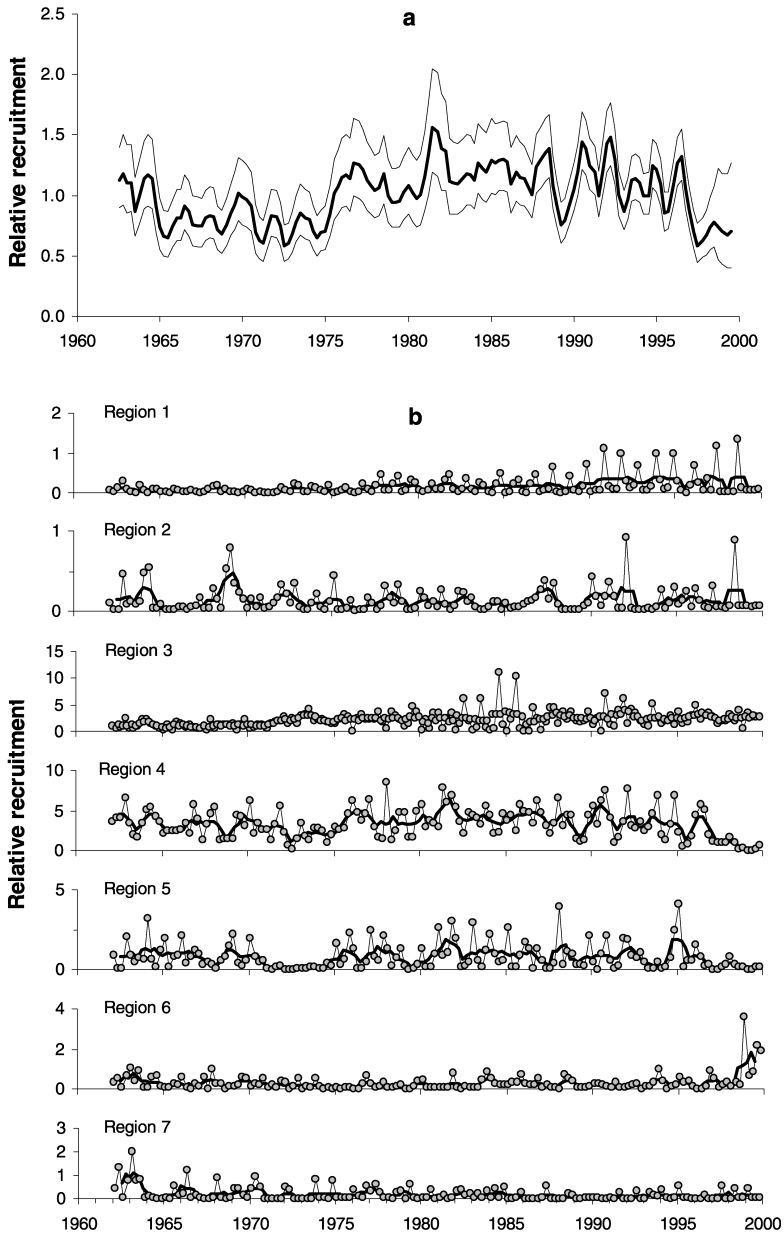

Fig. 18. (*a*) Average annual total recruitment with 95% confidence intervals and *(b)* quarterly recruitment (dots) by region; dark line in each regional plot is annual average recruitment.

integration of the posterior density using Monte Carlo Markov Chain and other simulation methods (Gelman *et al.* 1995). As faster computers become available, more flexible use of complex models will inevitably become feasible. Also, certain parts of the computer code appear amenable to multithreaded, distributed processing, which would allow a single model estimation to be run using the combined resources of several networked computers. This could greatly reduce the time required to run the model, and its application is currently under investigation.

The performance of the model applied to yellowfin tuna can be assessed in several ways. First, examination of the fits to the data included in the model provides a fundamental means of assessing performance. For yellowfin tuna, the fits to the catch, length-frequency and tagging data all appear to be good, and reveal no systematic failure of the model's assumptions. Secondly, we can use available exogenous data to test the validity of the model results. In this case, we have shown that the growth estimates arising from this model are very consistent with the results of counts of otolith daily

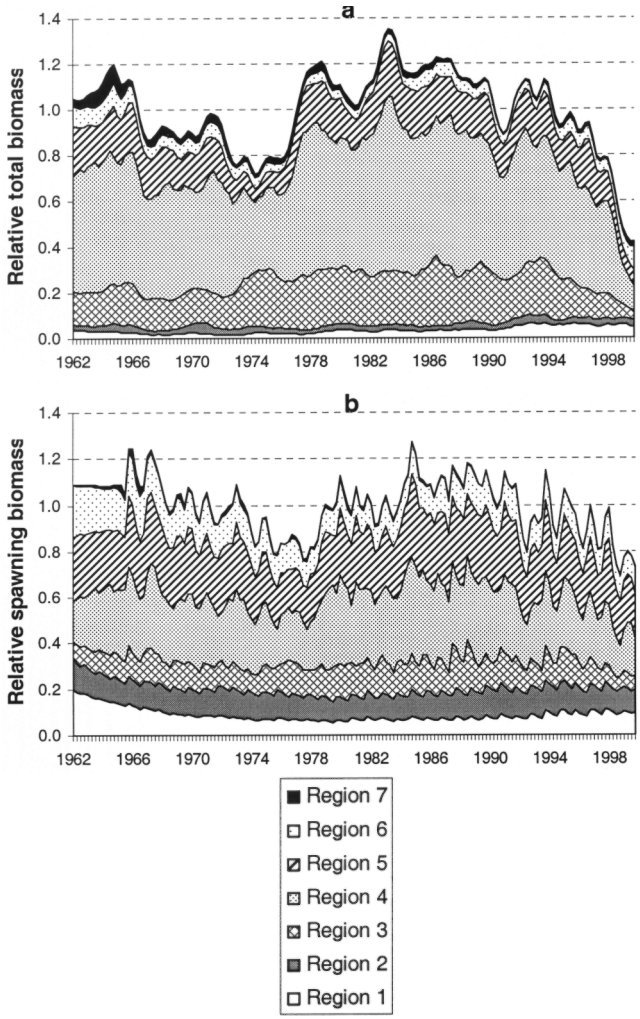

Fig. 19. Time series of estimated *(a)* relative total biomass and *(b)* relative spawning biomass, by region. The scale on the *y*-axis is relative to the 1962–99 average.

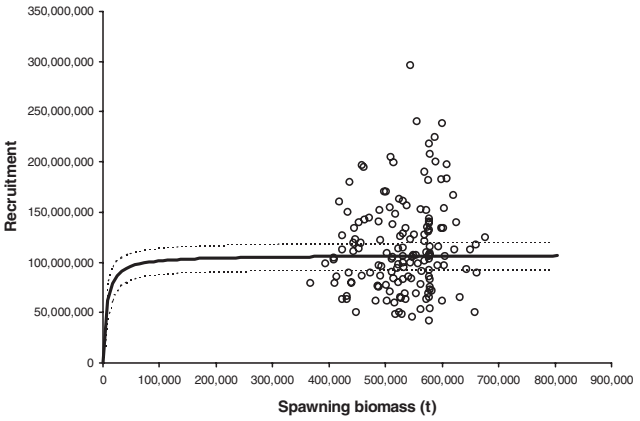

Fig. 20. Stock-recruitment relationship (solid line) and 95% confidence intervals (dotted lines) fitted to the estimates of spawning biomass and recruitment (circles).

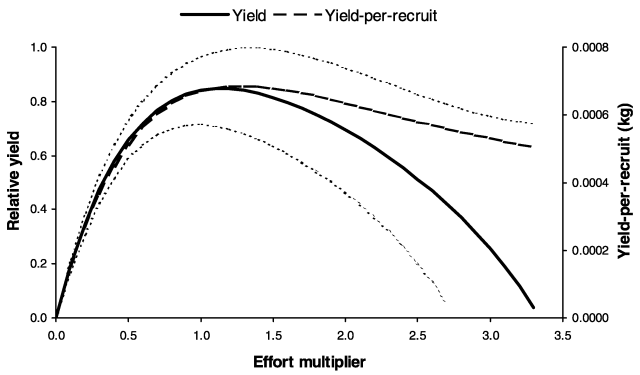

Fig. 21. Estimated yield curve with 95% confidence intervals (dotted lines). Yield-per-recruit curve shown for comparison.

rings. Thirdly, the model results must make good 'biological sense'. The yellowfin tuna model seems to fulfil this criterion in most respects.

Although the model is complex, it is nevertheless a gross simplification of reality in many respects. For example, growth is assumed to be identical among regions and constant over time. Movement and selectivity patterns are also assumed to be constant over time. As more powerful computers become available, it would be feasible to relax some of these assumptions as long as data were available to support a more complex parameterization. For example, allowing movement patterns to vary over time would likely require a long time series of tagging data. However, given that the end use of this and similar models is stock assessment, modelling every conceivable type of process variability is never likely to be feasible or necessary. Further research is required to better understand what level of model complexity is appropriate. We plan to address this question in the near future using simulated data obtained from an operational model designed to mimic the biology and fisheries for yellowfin tuna.

The yellowfin tuna analysis presented here falls somewhat short of a complete stock assessment, because various plausible alternatives to the base-case model structure are yet to be systematically tested. Alternative model structures that will soon be investigated include the following: time-series and regional variation in catchability for the longline fisheries; relaxation of the assumption of monotonically increasing selectivity with age for the longline fisheries; and the use of different penalty weights for some components of the objective function.

Although further work as outlined above is required, the results obtained to date have a number of possible implications for fisheries management. Recent declines in recruitment, although not obviously related to fishing activities, suggest that the productivity of the yellowfin stock may currently be lower than it has been previously. Recent catch levels appear to have been maintained by increases in fishing mortality, facilitated to a large

extent by technological advances (such as the use of FADs) in the purse-seine fishery. The yield analysis suggests that average catches over the past three years may have slightly exceeded the MSY. Some limitations on catch and/or fishing effort may therefore now be appropriate.

The results of the base-case model reveal strong regional differences in the impact of fishing. In particular, the fisheries in region 3 are estimated to have had a major effect on the sub-population in that region. Information on the Philippines and Indonesian domestic fisheries is poor (lack of effort data, limited length-frequency data), but the catches are relatively large and the estimated effects on populations are plausible. The effects on fisheries in regions 4 and 5, the major purse-seine fishing area, are also estimated to be considerable. In contrast, the fisheries in the sub-tropical regions appear to have had little effect on their respective sub-populations. Such heterogeneity in the fisheries and the impacts upon them will need to be considered when future management measures are designed.

Acknowledgments

We gratefully acknowledge the assistance of many colleagues participating in the Standing Committee on Tuna and Billfish who contributed data to and provided thoughtful comments on this work. We are especially grateful to Naozumi Miyabe of the Japan National Research Institute of Far Seas Fisheries for assistance in compiling Japanese longline data. We also thank Pierre Kleiber, who suggested the use of the implicit method for incorporating movement into the population dynamics. Funding assistance for this work was provided through Cooperative Agreement No. NA67RJ0154 from the National Oceanic and Atmospheric Administration. The views expressed herein are those of the authors and do not necessarily reflect the view of NOAA or any of its subagencies.

References

Anon. (2000). Multilateral high-level conference on the conservation and management of highly migratory fish stocks in the western and central Pacific Ocean. Seventh session. Honolulu, Hawaii, 30 August – 5 September, 2000.

Bertignac, M., Hampton, J., and Coan, A. A. (1999). Estimates of exploitation rates for north Pacific albacore, *Thunnus alalunga*, from tagging data. *Fishery Bulletin*, *US* **97**, 421–33.

Beverton, R. J. H., and Holt, S. J. (1957). On the dynamics of exploited fish populations. UK Ministry of Agriculture and Fisheries, Fishery Investigations (Ser. 2) No. 19.

Bigelow, K. A., Hampton, J., and Miyabe, N. (1999). Effective longline effort within the yellowfin habitat and standardized CPUE. 12th Standing Committee on Tuna and Billfish Working Paper YFT-3. (Secretariat of the Pacific Community: Noumea, New Caledonia.) 9 pp.

Doubleday, W. G. (1976). A least squares approach to analyzing catch at age data. *International Commission for Northwest Atlantic Fisheries Research Bulletin* **12**, 69–81.

Fournier, D., and Archibald, C. P. (1982). A general theory for analyzing catch at age data. *Canadian Journal of Fisheries and Aquatic Sciences* **39**, 1195–207.

Fournier, D. A., Sibert, J. R., Majkowski, J., and Hampton, J. (1990). MULTIFAN: a likelihood-based method for estimating growth parameters and age composition from multiple length frequency data sets illustrated using data for southern bluefin tuna (*Thunnus maccoyii*). *Canadian Journal of Fisheries and Aquatic Sciences* **47**, 301–17.

Fournier, D. A., Hampton, J., and Sibert, J. R. (1998). MULTIFAN-CL: a length-based, age-structured model for fisheries stock assessment, with application to South Pacific albacore, *Thunnus alalunga*. *Canadian Journal of Fisheries and Aquatic Sciences* **55**, 2105–16.

Gelman, A., Carlin, J. B., Stern, H. S., and Rubin, D. B. (1995). 'Bayesian Data Analysis.' (Chapman & Hall: London.) 526 pp.

Griewank, A., and Corliss, G. F. (Eds). (1991). Automatic differentiation of algorithms: theory, implementation, and application. (Society for Industrial and Applied Mathematics: Philadelphia, PA.)

Gudmundsson, G. (1994). Time-series analysis of catch-at-age observations. *Applied Statistics* **43**, 117–26.

Hampton, J. (1986). Effect of tagging on the condition of southern bluefin tuna, *Thunnus maccoyii* (Castlenau). *Australian Journal of Marine Freshwater Research* **38**, 699–705.

Hampton, J. (1997). Estimates of tag-reporting and tag-shedding rates in a large-scale tuna tagging experiment in the western tropical Pacific Ocean. *Fishery Bulletin*, *US* **95**, 68–79.

Hampton, J. (2000). Natural mortality rates in tropical tunas: size really does matter. *Canadian Journal of Fisheries and Aquatic Sciences* **57**, 1002–10.

Hampton, J., Lewis, A., and Williams, P. (1999). 'The western and central Pacific tuna fishery: 1998 overview and status of stocks.' Tuna Fisheries Assessment Report No. 1 (Secretariat of the Pacific Community: Noumea, New Caledonia.) 39 pp.

Hoenig, J. M, Barrowman, N. J., Pollock, K. H., Brooks, E. N., Hearn, W. S., and Polacheck, T. (1998). Models for tagging data that allow for incomplete mixing of newly tagged animals. *Canadian Journal of Fisheries and Aquatic Sciences* **55**, 1477–83.

Itano, D. G. (2000). The reproductive biology of yellowfin tuna (*Thunnus albacares*) in Hawaiian waters and the western tropical Pacific Ocean: project summary. SOEST 00–01 JIMAR Contribution 00–328 (Joint Institute of Marine and Atmospheric Research, University of Hawaii, Honolulu). 69 pp.

Kaltongga, B. (1998). Regional Tuna Tagging Project: data summary. Technical Report No. 35 (Oceanic Fisheries Programme, Secretariat of the Pacific Community: Noumea, New Caledonia.) 70 pp.

Lawson, T. A. (Ed.) (2000). Secretariat of the Pacific Community tuna fishery yearbook 1999. (Secretariat of the Pacific Community: Noumea, New Caledonia.)

Lehodey, P., and Leroy, B. (1998). Age and growth of yellowfin tuna (*Thunnus albacares*) from the western and central Pacific Ocean, as indicated by daily growth increments and tagging data. Working Paper No. 12, 11th Standing Committee on Tuna and Billfish. (Secretariat of the Pacific Community: Noumea, New Caledonia.)

Otter Research Ltd. (1994). Autodif: a C++ array extension with automatic differentiation for use in nonlinear modeling and statistics. (Otter Research Ltd: Nanaimo, Canada.)

Paloheimo, J. E. (1980). Estimation of mortality rates in fish populations. *Transactions of the American Fisheries Society* **109**, 378–86.

Press, W. H., Flannery, B. P., Teukolsky, S. A., and Vetterling, W. T. (1988). 'Numerical recipes in C.' (Cambridge University Press: New York.) 994 pp.

Schaefer, K. M. (1996). Spawning time, frequency, and batch fecundity of yellowfin tuna, *Thunnus albacares*, near Clipperton Atoll in the eastern Pacific Ocean. *Fishery Bulletin US* **94**, 98–112.

Schaefer, K. M. (1998). Reproductive biology of yellowfin tuna (*Thunnus albacares*) in the eastern Pacific Ocean. *Bulletin of the Inter-American Tropical Tuna Commission* **21**, 205–72.

Schnute, J., and Fournier, D. A. (1980). A new approach to length frequency analysis: growth structure. *Journal of the Fisheries Research Board of Canada* **37**, 1337–51.

Schnute, J. T., and Richards, L. J. (1998). Analytical models for fishery reference points. *Canadian Journal of Fisheries and Aquatic Sciences* **55**, 515–28.

Seber, G. A. F. (1973). 'The Estimation of Animal Abundance and Related Parameters.' (Griffin: London.) 506 pp.

Ward, R. D., Elliott, N. G., and Grewe, P. M. (1994). Allozyme and mitochondrial DNA variation in yellowfin tuna (*Thunnus albacares*) from the Pacific Ocean. *Marine Biology* **118**, 531–9.

Manuscript received 30 March 2001; revised and accepted 6 July 2001

Appendix A. Population dynamics model for yellowfin tuna

Age-structured dynamics

The equations governing the general age-structured dynamics of yellowfin tuna are:

$$N'_{atr} = \begin{cases} \bar{R}\exp(\varphi_t)\alpha_r\gamma_{tr} & a = 1; 1 \le t \le T \\ N'_{a1r} & 1 < a \le A; t = 1 \\ \exp(-Z_{a-1,t-1,r})N_{a-1,t-1,r} & 1 < a < A; 1 < t \le T \\ \exp(-Z_{a-1,t-1,r})N_{a-1,t-1,r} + \exp(-Z_{a,t-1,r})N_{a,t-1,r} & a = A; 1 < t \le T \end{cases} \quad \text{(A.1)}$$

$$Z_{atr} = \sum_{f_r} F_{at f_r} + M_a; \quad \text{(A.2)}$$

where

N'_{atr} is the number of age-class a fish at the beginning of time period t in region r before movement has taken place,
N_{atr} is the number of age-class a fish at the beginning of time period t in region r after movement has taken place,
$\bar{R}$ is the spatially aggregated, average recruitment,
φ_t is a normally distributed random variable, $\varphi_t \sim N(0;\sigma_r^2)$, determining the deviation of the spatially aggregated recruitment in time period t from its average,
α_r denotes the average distribution of recruitment among regions,
γ_{tr} specifies the spatial distribution of recruitment in time period t,
A is the total number of age-classes,
T is the total number of quarterly time periods,
Z_{atr} is the instantaneous rate of total mortality of age-class a during time period t in region r,
F_{atf_r} is the instantaneous rate of fishing mortality of age-class a during time period t by fishery f_r occurring in region r, and
M_a is the instantaneous rate of natural mortality of age-class a.

The recruitment parameters are subject to the constraints that: $\varphi_t \sim N(0;\sigma_r^2)$; $\sum_t \varphi_t = 0$; $\sum_r \alpha_r = 1$; $\prod_t \gamma_{tr} = 1$; and $\sum_r \alpha_r\gamma_{tr} = 1$.

The initial population N'_{alr} is parameterized as a function of the average spatially disaggregated recruitment $\bar{N}'_{1r}$ and average total mortality $\bar{Z}_{ar}$:

$$N'_{a1r} = \begin{cases} \exp\left[-\sum_{a'<a} \bar{Z}_{a'r}\right]\bar{N}'_{1r} & 1 < a < A \\ \dfrac{\bar{N}'_{1r}}{1-\exp(-\bar{Z}_{ar})}\exp\left[-\sum_{a'<a} \bar{Z}_{a'r}\right] & a = A \end{cases}$$

$$\bar{N}'_{1r} = \frac{1}{(k-1)}\sum_{t=2}^{t=k} N'_{1tr}$$

$$\bar{Z}_{ar} = \frac{1}{(k-1)}\sum_{t=2}^{t=k} Z_{atr} \quad \text{(A.3)}$$

where k is the last time period (20 for the yellowfin tuna analysis) included in the average.

Movement is assumed to occur instantaneously at the beginning of each time period. Let $\mathbf{N'_{at}}$ and $\mathbf{N_{at}}$ denote vectors equivalent to N'_{atr}, and N_{atr}, $r = 1, \ldots, 7$. $\mathbf{N'_{at}}$ is transformed to $\mathbf{N_{at}}$ by an age-specific movement transition matrix, $\mathbf{B_a}$:

$$\mathbf{N_{at}} = \mathbf{B_a^{-1}} \cdot \mathbf{N'_{at}}; \tag{A.4}$$

$$\mathbf{B_a} = \begin{bmatrix} 1+\nu_a^{12}+\nu_a^{13}+\nu_a^{14} & -\nu_a^{21} & -\nu_a^{31} & -\nu_a^{41} & 0 & 0 & 0 \\ -\nu_a^{12} & 1+\nu_a^{21}+\nu_a^{25} & 0 & 0 & -\nu_a^{52} & 0 & 0 \\ -\nu_a^{13} & 0 & 1+\nu_a^{31}+\nu_a^{34} & -\nu_a^{43} & 0 & 0 & 0 \\ -\nu_a^{14} & 0 & -\nu_a^{34} & 1+\nu_a^{41}+\nu_a^{43}+\nu_a^{45}+\nu_a^{46} & -\nu_a^{54} & -\nu_a^{64} & 0 \\ 0 & -\nu_a^{25} & 0 & -\nu_a^{45} & 1+\nu_a^{52}+\nu_a^{54}+\nu_a^{57} & 0 & -\nu_a^{75} \\ 0 & 0 & 0 & -\nu_a^{46} & 0 & 1+\nu_a^{64}+\nu_a^{67} & -\nu_a^{76} \\ 0 & 0 & 0 & 0 & -\nu_a^{57} & -\nu_a^{67} & 1+\nu_a^{75}+\nu_a^{76} \end{bmatrix} \tag{A.5}$$

where ν_a^{xy} denotes the probability of movement of an age-class a fish from region x to region y. Note that Eqns (A.4) and (A.5) utilize the fully-implicit, or backward-time method of solving the finite difference equation for movement (see Press *et al.* 1988 for a good discussion of implicit differencing), which guarantees numerical stability even with large rates of movement. The zero elements of $\mathbf{B_a}$ represent non-adjacent regions while the remaining non-diagonal elements are the movement coefficients to be estimated. One outcome of the implicit method is that fish may move between any two non-adjacent regions in a single time step as long as the regions are linked by one or more other regions that are adjacent.

Age dependency of ν_a^{xy} is specified using a flexible function that can result in increasing ($\phi_1^{xy} > 0$), decreasing ($\phi_1^{xy} < 0$) or constant ($\phi_1^{xy} = 0$) movement coefficients with increasing age:

$$\nu_a^{xy} = \phi_0^{xy} \exp\left(\phi_1^{xy} \kappa_a\right) \tag{A.6}$$

where ϕ_0^{xy} and ϕ_1^{xy} are the parameters to be estimated, while κ_a expresses age scaled between –1 and 1.

The catch in numbers of age-class a fish during time period t by a fishery f_r occurring in region r is given by:

$$C_{at f_r} = \frac{F_{at f_r}}{Z_{atr}} [1 - \exp(-Z_{atr})] N_{atr}. \tag{A.7}$$

Parameterization of fishing mortality

Fishing mortality is parameterized as:

$$\log(F_{at f_r}) = \log(s_{a f_r}) + \log(q_{t f_r}) + \log(E_{t f_r}) + \varepsilon_{t f_r} \tag{A.8}$$

where

s_{afr} is the selectivity coefficient for age-class a for fishery f_r,

q_{tfr} is the catchability coefficient for fishery f_r during time period t,

E_{tfr} is the fishing effort for fishery f_r during time period t, and

ε_{tfr} is a robustified, normally distributed random variable, $\varepsilon_{tfr} \sim N(0;\sigma^2\varepsilon_{fr})$, representing relatively large transient deviations in the effort – fishing mortality relationship (or simply, effort deviations).

A smoothing transformation is applied to the selectivity coefficients to account for the degree of length overlap between adjacent age-classes. Let μ_a and σ_a denote the mean length and standard deviation of age-class a fish (assumed to be normally distributed) and let Ω be a function such that $\Omega^{-1}(\mu_a) = a$. Then, $\Omega^{-1}(\mu_a+\delta_k\sigma_a) = i_{ak}+z_{ak}$, where i_{ak} is the integer component of the age, $0 \le z_{ak} < 1$ is the fractional component of the age and δ_k is a vector of points sampling the normal distribution of length-at-age, expressed in units of standard deviations from the mean:

$$\delta_k = [-1.5\ -1.0\ -0.5\ -0.25\ 0\ 0.25\ 0.5\ 1.0\ 1.5] \quad k = -4, -3, \ldots, 3, 4. \tag{A.9}$$

Then:

$$s_{af_r} = \sum_{k=-4}^{4} \omega_k \left[s'_{i_{ak} f_r} \left(1 - z_{ak}\right) + s'_{i_{ak}+1, f_r} \, z_{ak} \right] \tag{A.10}$$

where
$s'_{i_{ak} f_r}$ is the purely age-based selectivity coefficient,
s_{af_r} is the length-smoothed selectivity coefficient, and
ω_k are weights that are simple approximations to integrals of the normal distribution:

$$\omega_k = h_k \Big/ \left(h_0 + 2h_1 + 2h_2 + 2h_3 + 2h_4\right); \tag{A.11}$$

$$h_k = \begin{cases} \exp\left(-\delta_k \cdot \delta_k / 2\right) & k = -2, -1, 0, 1, 2 \\ 2\exp\left(-\delta_k \cdot \delta_k / 2\right) & k = -4, -3, 3, 4. \end{cases} \tag{A.12}$$

Time-series structure in catchability is allowed by:

$$\log\left(q_{y+1, f_r}\right) = \log\left(q_{y f_r}\right) + \eta_{y f_r} \tag{A.13}$$

where η_{yf_r} is a normally distributed random variable, $\eta_{yf_r} \sim N(0;\sigma^2_{\eta_{f_r}})$, representing small, cumulative changes in catchability (or catchability deviations) that we assume occur at regular intervals (y), in this case every three years. Within a year, catchability is allowed to vary with a regular seasonal pattern:

$$\log\left(q_{y f_r}\right) = \log\left(q'_{y f_r}\right) + c_{1 f_r} \sin\left[2\pi \left(\upsilon_t \Big/ 4 - c_{2 f_r}\right)\right] \tag{A.14}$$

where
q'_{yf_r} is the catchability coefficient before seasonal adjustment,
υ_t is an integer (1–4) denoting the quarter of the year pertaining to time period t,
c_{1f_r} is the fishery-specific amplitude parameter, and
c_{2f_r} is the fishery-specific phase parameter.

Modelling the length-frequency data

We assume that the lengths of age-class a fish comprising a (random) length-frequency sample of the catch of fishery f_r in time period t are normally distributed about their mean μ_a with standard deviation σ_a. Then, the probability q_{ia} that an age-class a fish selected at random from such a length-frequency sample lies in length interval i is:

$$q_{ia}\left(\mu_a, \sigma_a\right) \approx \frac{w}{\sqrt{2\pi}\,\sigma_a} \exp\left\{ \frac{-\left(x_i - \mu_a\right)^2}{2\sigma_a^2} \right\} \tag{A.15}$$

where
w is the width of the length intervals, and
x_i is the mid-point of the ith length interval.

Note that this is an approximation to integrating over the length range $(x_i - w/2,\ \ x_i + w/2)$ and is adequate as long as $\sigma_a > w$ (Fournier *et al*. 1990). Then, the expected proportion of a length-frequency sample taken from fishery f_r during time period t occurring in length interval i is:

$$Q^{\text{pred}}_{it f_r} = \sum_{a=1}^{A} p_{at f_r} \, q_{ia} \tag{A.16}$$

where p_{atf_r} is the expected proportion of age-class a fish in the length-frequency sample. p_{atf_r} is related to predictions from the age-structured dynamics by:

$$p_{at f_r} = \frac{C_{at f_r}}{\sum_{a=1}^{A} C_{at f_r}} \tag{A.17}$$

The mean lengths μ_a are independent model parameters for $a = 2–8$ with $\mu_{a+1} \geq \mu_a$. For $a = 9–20$,

$$\mu_a = L_1 + (L_A - L_1)\left\{\frac{1-\rho^{a-1}}{1-\rho^{A-1}}\right\} \tag{A.18}$$

where
L_1 is the mean length of the first age-class,
L_A is the mean length of the last age-class, and
ρ is the Brody growth coefficient (Schnute and Fournier 1980; Fournier *et al.* 1990).

Following Fournier *et al.* (1990, 1998), the standard deviation of length-at-age is assumed to be a simple linear function of length involving two parameters λ_1 and λ_2:

$$\sigma_a = \lambda_1 \exp\left\{\lambda_2\left[-1+2\left(\frac{1-\rho^{a-1}}{1-\rho^{A-1}}\right)\right]\right\}. \tag{A.19}$$

λ_1 determines the magnitude of the standard deviations and λ_2 determines the length-dependent trend. If $\lambda_2 = 0$, the standard deviations are length-independent.

Estimation of spawning biomass

The spawning biomass of the population is defined as:

$$SB_{tr} = \sum_{a=1}^{A} N_{atr}\, S_a W_a; \tag{A.20}$$

$$W_a = n\left(\mu_a^3 + 3\mu_a\sigma_a^2\right) \tag{A.21}$$

where
SB_{tr} is the spawning biomass at the beginning of time period t in region r,
S_a is the proportion of age-class a fish that are reproductively mature,
W_a is the mean weight of age-class a fish and
n is the scaling coefficient in the weight–length relationship $W = nL^3$.

Estimates of S_a were obtained from Itano (2000), while n was estimated from yellowfin tuna weight–length observations (Secretariat of the Pacific Community, unpublished).

Appendix B. Population dynamics model for tagged yellowfin tuna

The dynamics of tagged yellowfin tuna are governed by equations analogous to Eqns A.1 through A.15, and the parameters for the tagged fish (or simply tags, for short) and the general population are shared. The major modifications necessary for modelling the tags are that recruitment is replaced by tag releases and that the tags are stratified by release cohorts. Let a cohort, c, of tags be defined as a group of fish in age-class $a = a_c^{rel}$ released during time interval $t = t_c^{rel}$ in region r. Then, the equation for tags analogous to Eqn A1 is:

$$Ntag'_{catr} = \begin{cases} Ntag'_{ca_c^{rel}t_c^{rel}r} & a = a_c^{rel};\ t = t_c^{rel} \\ \exp\left(-Z_{a-1,t-1,r}\right) Ntag_{c,a-1,t-1,r} & a_c^{rel} < a < A \\ \exp\left(-Z_{a-1,t-1,r}\right) Ntag_{c,a-1,t-1,r} + \exp\left(-Z_{a,t-1,r}\right) Ntag_{ca,t-1,r} & a = A \end{cases} \tag{B.1}$$

$$Z_{atr} = \sum_{f_r} F_{atf_r} + M_a \tag{B.2}$$

where

$Ntag'_{catr}$ is the population of tags from release cohort c in age-class a at the start of time period t in region r before movement has taken place, and

$Ntag_{catr}$ is the corresponding population after movement has taken place.

The ages-at-release of tags a_c^{rel} are not known and must be estimated from the lengths-at-release. We adopted a procedure in which tag releases with length l are distributed to age-classes based on the approximate age-distribution of length l estimated from the mean length- and standard deviation-at-age estimates at each function evaluation.

The numbers of tag recaptures $Ctag^{\text{pred}}_{catf_r}$, by cohort, age-class, time period and fishery are predicted by an equation analogous to Eqn (A.7):

$$Ctag^{\text{pred}}_{catf_r} = \frac{F_{atf_r}}{Z_{atr}}[\,1-\exp(-Z_{atr})\,]\;Tag_{catr}\;X_{f_r} \tag{B.3}$$

where X_{f_r} is the rate of tag reporting for fishery f_r.

Because the fishing mortality for the tags is thus far assumed to be identical to that for the population in general, we are assuming implicitly that the probability of capturing a tag is the same as that of an untagged fish. This assumption may be violated soon after release, before the tags have had a chance to mix thoroughly with the untagged population. To correct for this, we compute cohort-specific fishing mortality rates F'_{catf_r} for the tags for m time periods after release. F'_{catf_r} is determined by solving Eqn (B.3) using the Newton-Raphson technique (see Press *et al*. 1988 for details) after setting $Ctag^{\text{pred}}_{catf_r} = Ctag^{\text{obs}}_{catf_r}$ for the initial m time periods. Then, the substitution of F'_{catf_r} into Eqn (B.2), and similarly Z'_{catf_r} into Eqn (B.1) ensures that the tagged population is correctly discounted for anomalous recaptures of recent releases. We judged that m = 1 was sufficient to deal with problems of non-mixing of recent yellowfin tuna releases.

The movement dynamics and the parameterization of catchability and selectivity for the tagged population are as described for the untagged population in Appendix A.

Appendix C. Log-likelihood functions

Total catch data

The objective function contribution for the observed total catches is given by:

$$\Theta_c = p_c \sum_t \sum_{f_r} \left\{ \log\left(1+C^{\text{obs}}_{tf_r}\right) - \log\left(1+C^{\text{pred}}_{tf_r}\right) \right\}^2; \tag{C.1}$$

$$C^{\text{pred}}_{tf_r} = \sum_{a=1}^{A} C_{atf_r} \text{ for fisheries with catches expressed in numbers of fish and} \tag{C.2}$$

$$C^{\text{pred}}_{tf_r} = \sum_{a=1}^{A} C_{atf_r} W_a \text{ for fisheries with catches expressed in weight.} \tag{C.3}$$

The weighting factor p_c is determined by the prior assumption made about the accuracy of the observed total catch data. For yellowfin tuna catches, we assumed that p_c = 100, which is equivalent to a residual s.d. of approximately 0.07. In other words, we assume that the catches are observed with relatively little error.

Length-frequency data

Due to the large variability that commonly occurs in length-frequency data, the use of a robust likelihood function is essential. The rationale and technicalities of this procedure are outlined in Fournier *et al.* (1990). They derived a robust log-likelihood function based on an assumed normal distribution of $Q^{\text{obs}}_{itf_r}$, the observed proportion of a length-frequency sample, taken from fishery f_r during time period t, occurring in length interval i, and showed that this function is approximately equal to a self-scaling, robustified, minimum χ^2 statistic. The contribution of the length-frequency data to the objective function is therefore:

$$\Theta_L = 0.5 \sum_i \sum_t \sum_{f_r} \log\left[2\pi\left(\xi_{i,t,f_r}+1/I\right)\right] + I \sum_t \sum_{f_r} \log\left(\tau_{t f_r}\right)$$

$$- \sum_i \sum_t \sum_{f_r} \log\left\{\exp\left[\frac{-\left(Q^{\text{obs}}_{it f_r} - Q^{\text{pred}}_{it f_r}\right)^2}{2\left(\xi_{it f_r}+1/I\right)\tau^2_{t f_r}}\right] + 0.001\right\}; \tag{C.4}$$

$$\xi_{it f_r} = Q^{\text{obs}}_{it f_r}\left(1 - Q^{\text{obs}}_{it f_r}\right); \tag{C.5}$$

$$\tau^2_{t f_r} = p_L \Big/ \min\left(S_{t f_r}, 1000\right) \tag{C.6}$$

where

S_{tf_r} is the size of the length-frequency sample taken from fishery f_r during time period t,

I is the number of length intervals in the samples, and

P_L is a multiplier, set equal to 10 for the yellowfin tuna analysis, that recognizes that the variance of real length-frequency samples is almost certainly much greater than truly random samples of a given size.

The term $\min(S_{tf_r}, 1000)$ reduces the influence of very large sample sizes by assuming that sample sizes of >1000 are no more accurate than sample sizes of 1000. The constant $1/I$ ensures that the variance term is not zero when $Q^{\text{obs}}_{itf_r} = 0$, rendering the model less sensitive to occasional observations of low probability. The addition of the constant 0.001 provides additional robustness to the estimation. Note that, in contrast to Fournier *et al.* (1990), the variance ζ_{itf_r} is based on $Q^{\text{obs}}_{itf_r}$ rather than $Q^{\text{pred}}_{itf_r}$. This change was introduced after analyses of simulated data (Secretariat of the Pacific Community, unpublished) suggested that better model performance was obtained by using $Q^{\text{obs}}_{itf_r}$ to compute the variance term.

Tagging data

The likelihood functions that are most commonly used to model tagging data are the multinomial and the Poisson. However, a problem common to both of these statistical models is that the variance is heavily constrained by the mean; typically, tagging data are more variable than predicted because the recaptures of tagged fish are not completely independent events, which is an assumption of these models. We have dealt with this problem by using the negative binomial distribution as the basis of the likelihood function for the tagging data. The negative binomial allows the mean and variance to be fitted separately, with the variance at least as great as the mean (Gelman et al. 1995). This model has the flexibility to allow greater variability in the data than the Poisson model (which is its limiting case), and can therefore be considered as an overdispersed and robust alternative to the Poisson for modelling tagging data. The general formulation of the negative binomial is:

$$p(\theta) = \binom{\theta+\alpha-1}{\alpha-1}\left(\frac{\beta}{\beta+1}\right)^{\alpha}\left(\frac{1}{\beta+1}\right)^{\theta} \quad \theta = 0, 1, 2, \ldots$$

$$\mathrm{E}(\theta) = \frac{\alpha}{\beta}; \quad \mathrm{var}(\theta) = \frac{\alpha}{\beta^2}(\beta+1) \tag{C.7}$$

where θ is a negative binomial random variable and α and β are parameters. The use of the negative binomial in this context is somewhat different to the normal usage where the data consist of multiple observations with constant $\mathrm{E}(\theta)$. Here, our data consist of single observations of tag return numbers from many strata each having a unique $\mathrm{E}(\theta)$, which requires a different parameterization. The variance and coefficient of variation can be written in terms of one of the coefficients (say, α) and $\mathrm{E}(\theta)$:

$$\mathrm{var}(\theta) = \mathrm{E}(\theta)\left[1 + \frac{\mathrm{E}(\theta)}{\alpha}\right]; \; \mathrm{CV}(\theta) = \mathrm{E}(\theta)^{-1/2}\left[1 + \frac{\mathrm{E}(\theta)}{\alpha}\right]^{1/2}. \tag{C.8}$$

Let α be a function of $E(\theta)$ and a constant ϖ, which results in

$$\mathrm{CV}(\theta) = \mathrm{E}(\theta)^{-1/2}\left[1+\frac{1}{\varpi}\right]^{1/2};$$
$$\alpha = \varpi\,\mathrm{E}(\theta) \quad (\varpi > 0). \tag{C.9}$$

Note that $E(\theta)^{-1/2}$ is the CV for a Poisson distribution; therefore the multiplicative term $[1+\frac{1}{\varpi}]^{1/2}$ represents the degree to which the Poisson CV is expanded for overdispersion ($CV(\theta)\rightarrow E(\theta)^{-1/2}$ as $\varpi\rightarrow\infty$).

Expressing ϖ as a fishery-specific parameter, the negative binomial likelihood function for the tagging data is:

$$\ell_T = \prod_{cat\,f_r'} \frac{\left(Ctag^{\mathrm{obs}}_{cat\,f_r'} + \alpha_{cat\,f_r'} - 1\right)!}{\left(\alpha_{cat\,f_r'} - 1\right)!\,Ctag^{\mathrm{obs}}_{cat\,f_r'}!}\left(\frac{\alpha_{cat\,f_r'}}{\alpha_{cat\,f_r'} + Ctag^{\mathrm{pred}}_{cat\,f_r'}}\right)^{\alpha_{cat\,f_r'}}$$
$$\left(\frac{Ctag^{\mathrm{pred}}_{cat\,f_r'}}{\alpha_{cat\,f_r'} + Ctag^{\mathrm{pred}}_{cat\,f_r'}}\right)^{Ctag^{\mathrm{obs}}_{cat\,f_r'}};$$
$$\alpha_{cat\,f_r'} = \varpi_{f_r'}\,Ctag^{\mathrm{pred}}_{cat\,f_r'} \tag{C.10}$$

where the subscript f_r' represents the fisheries grouped for the purposes of the tag recaptures and $\varpi_{f_r'}$ is the set of variance-determining parameters (one for each fishery group) to be estimated. Taking the negative log of Eqn (C.10) and employing the log-gamma approximation for factorial terms (Press *et al*. 1988) gives the contribution of the tagging data to the objective function:

$$\Theta_T = -\sum_{cat\,f_r'} \log\Gamma\left(Ctag^{\mathrm{obs}}_{cat\,f_r'} + \alpha_{cat\,f_r'}\right) - \log\Gamma\left(\alpha_{cat\,f_r'}\right) - \log\Gamma\left(Ctag^{\mathrm{obs}}_{cat\,f_r'} + 1\right)$$
$$+ \alpha_{cat\,f_r'}\left[\log\left(\alpha_{cat\,f_r'}\right) - \log\left(\alpha_{cat\,f_r'} + Ctag^{\mathrm{pred}}_{cat\,f_r'}\right)\right]$$
$$+ Ctag^{\mathrm{obs}}_{cat\,f_r'}\left[\log\left(Ctag^{\mathrm{pred}}_{cat\,f_r'}\right) - \log\left(\alpha_{cat\,f_r'} + Ctag^{\mathrm{pred}}_{cat\,f_r'}\right)\right]. \tag{C.11}$$

Appendix D. Priors and penalties

Priors and smoothing penalties are used to constrain the parameterization of the model. Priors or penalties that result in non-trivial contributions to the objective function in the reference analysis are described below.

Effort deviations

The prior distributions for the effort deviations ε_{tf_r} (Eqn A.8) are assumed to be a mixture of a normal distribution with zero mean and the variances related to the constants $p_{\varepsilon f_r}$, and a 'contaminating' distribution to increase the probability of observations in the tails of the normal distribution. The contribution to the objective function of the prior for the effort deviations is:

$$\Theta_\varepsilon = -\sum_{f_r}\sum_{t} \log\left[\exp\left(-p_{\varepsilon f_r}\sqrt{E_{t f_r}}\,\varepsilon^2_{t f_r}\right) + 0.05\exp\left(-\frac{p_{\varepsilon f_r}\sqrt{E_{t f_r}}}{5}\varepsilon^2_{t f_r}\right)\right]. \tag{D.1}$$

The second term within the square brackets is the overdispersion term to enhance robustness. Note that the ε_{tf_r} are weighted by a fishery-specific weight $p_{\varepsilon f_r}$, and by the square root of the normalized effort for that time period. This ensures that observations of very low effort have relatively little impact on the objective function through the effort deviations. The generic weight $p_{\varepsilon f_r}$ is related to the variance $\sigma^2_{\varepsilon f_r}$ of ε_{tf_r} at average effort:

$$p_{\varepsilon f_r} = \frac{1}{2\sigma^2_{\varepsilon f_r}}. \tag{D.2}$$

Therefore, a relatively high value of $p_{\varepsilon f_r}$ results in small deviations from the observed effort while a relatively small value of $p_{\varepsilon f_r}$ allows the model greater flexibility to deviate from the observed effort data if this results in a better overall fit to the total data. For the yellowfin tuna analysis, effort data were not available for the PR, PH and IN fisheries. In this case we made the minimal assumption that effort was constant, but set $p_{\varepsilon f_r}$ to 1 (CV of $\exp(\varepsilon_{.f_r}) \approx 0.80$) to allow the model to, in effect, estimate the effort for these fisheries most consistent with the overall data. For the purse seine fisheries, we assumed that effort estimates were less reliable than those for the longline fisheries, hence we set $p_{\varepsilon f_r}$ for the purse seine fisheries to 10 (CV of $\exp(\varepsilon_{.f_r}) \approx 0.22$) at the average level of effort) and for the longline fisheries to 100 (CV of $\exp(\varepsilon_{.f_r}) \approx 0.07$) at the average level of effort). This relatively low level of variability for the longline fisheries was assumed because the longline effort data were pre-standardized using a habitat model. Note that these assumptions regarding variability only refer to the normal component of the effort-deviation priors. The prior probabilities are also influenced by the overdispersion term in Eqn (D.1).

Catchability deviations

The prior distributions of the catchability deviations η_{yf_r} (Eqn A.14) are assumed to be normally distributed with mean $\mu_{\eta f_r}$ and with the variance determined by the constant $p_{\eta f_r}$. The contribution to the objective function is:

$$\Theta_\eta = \sum_{f_r} p_{\eta f_r} \sum_y \left(\mu_{\eta f_r} - \eta_{y f_r}\right)^2 \tag{D.3}$$

The constants $p_{\eta f_r}$ were set at 50 (CV of $\exp(\eta_{.f_r}) \approx 0.10$) for all purse seine fisheries. For the PR, PH and IN fisheries, $p_{\eta f_r}$ was set to 1 (CV of $\exp(\eta_{.f_r}) \approx 0.80$) in order to allow maximum flexibility to estimate catchability where an assumption about fishing effort was required. The means $\mu_{\eta f_r}$ of the prior distributions were set to zero. Catchability deviations were fixed at zero for the longline fisheries, consistent with an assumption of constant catchability.

Seasonal catchability

The seasonal catchability amplitude parameter c_{1f_r} has a prior distribution that is normally distributed with a mean of zero and variance determined by the constant $p_s = 0.1$. The contribution to the objective function is:

$$\Theta_s = p_s c^2_{1f_r}. \tag{D.4}$$

Recruitment deviations

The spatially aggregated recruitment deviations φ_t are assumed to be normally distributed with zero mean and a variance determined by the constant p_φ. We also assume a small amount of auto-correlation in the recruitment deviations. The contribution to the objective function of the prior for the recruitment time-series deviations is:

$$\Theta_\varphi = p_\varphi \sum_t \varphi_t^2 + 0.1 \sum_{t=1}^{T-4} \left(\varphi_{t+4} - \varphi_t\right)^2. \tag{D.5}$$

The weight p_φ is set to a small value (1.4) in order to allow relatively large variance for φ_t (resulting in a spatially aggregated recruitment variation of about one-third to three times the average). The second term of Eqn (D.5) introduces a small penalty on the difference between recruitment deviations in the same quarter of successive years, thus providing a small amount of auto-correlation in the φ_t.

We also apply a small penalty on deviations of spatially aggregated recruitment, $\bar{R}\varphi_t$, from that predicted by the stock-recruitment relationship. Let R'_t be the spatially aggregated equilibrium recruitment resulting from the spatially aggregated spawning biomass, SB_{t-l}, where l is the lag between spawning and recruitment (assumed to be three months for yellowfin tuna). We use the Beverton and Holt (1957) stock-recruitment relationship:

$$R'_t = \frac{\alpha' SB_{t-l}}{\beta' + SB_{t-l}} \tag{D.6}$$

where α' and β' are the stock-recruitment parameters. The asymptotic recruitment parameter α' is determined analytically, while β' is estimated as a model parameter. The penalty for deviations from R'_t is given by:

$$\Theta_{sb} = p_{sb} \sum_{t=l+1}^{T} [\log(\bar{R}\varphi_t) - \log(R'_t)]^2 \tag{D.7}$$

where $p_{sb} = 1$ allows relatively large deviations to occur.

The time-series deviations from the average spatial distribution of recruitment, $\gamma_{t,r}$, are assigned weak prior distributions of mean zero. The contribution of this prior to the objective function is:

$$\Theta_{\gamma} = p_{\gamma} \sum_{t} \sum_{r} [\log(\gamma_{tr})]^2 \tag{D.8}$$

where $p_{\gamma} = 0.1$.

Movement coefficients

The prior distributions of the movement parameters ϕ_0^{xy} and ϕ_1^{xy} have zero mean and a relatively high s.d. (~0.3):

$$\Theta_{\phi} = p_{\phi}[\sum_{x,y} (\phi_0^{x,y})^2 + (\phi_1^{x,y})^2]. \tag{D.9}$$

where $p_{\phi} = 5$. The effect of these priors is that, in the absence of any information in the data regarding movement into or out of a particular region, movement will tend towards zero.

Tag-reporting rates

The prior distributions for the tag-reporting rates are fishery-specific and are based in some cases on the results of tag-seeding experiments (Hampton 1997). The contribution of the reporting-rate priors is:

$$\Theta_{\Gamma} = \sum_{f_r} p_{f_r} (X_{f_r} - \mu_{f_r})^2 \tag{D.10}$$

where p_{f_r} is determined by the reporting rate variance and μ_{f_r} is the mean of the prior distribution of the reporting rate. For the non-longline fisheries (fisheries 1–9), we specified the prior distributions according to estimates of reporting rates and their variability obtained by Hampton (1997). For the longline fisheries, relatively uninformative priors with high variance were specified, thus allowing the longline fishery reporting rates to be determined largely by the model data. Details of the reporting rate priors are given in Table D1.

Table D1. Tag-reporting rate prior distributions

Fishery	Mean	Standard deviation	p_{f_r}
Philippines and Indonesia domestic	0.80	0.07	100
Purse seine	0.59	0.05	234
Longline	0.50	0.17	17

Selectivity curvature

Selectivity curvature is constrained by a penalty based on the second and third differences of the selectivity coefficients:

$$\Theta_s = \sum_{f_r} p_{s_1} \sum_{a=1}^{A-2} (s_{a f_r} - 2s_{a+1,f_r} + s_{a+2,f_r})^2 + p_{s_2} \sum_{a=1}^{A-3} (s_{a f_r} - 3s_{a+1,f_r} + 3s_{a+2,f_r} - s_{a+3,f_r})^2 \tag{D.11}$$

where p_{s_1} and p_{s_2} are set to 0.001.

Natural mortality rates

The natural mortality rates M_a are constrained by moderate smoothing penalties to avoid large changes in M_a between successive age classes and extreme deviation from the mean. These smoothing penalties are:

$$\Theta_M = p_{M_1} \sum_{a=1}^{A-2} (M'_a - 2M'_{a+1} + M'_{a+2})^2 + p_{M_2} \sum_{a=1}^{A-1} (M'_a - M'_{a+1})^2 + p_{M_3} \sum_{a=1}^{A} (M'_a)^2 \tag{D.12}$$

where $M'_a = \log(M_a) - \sum_a \log(M_a)/A$ and p_{M_1}, p_{M_2} and p_{M_3} are weights equal to 25, 5 and 10, respectively.

Appendix E. Estimated parameters, priors and other constraints for the yellowfin tuna model

Parameter category	Symbol	Number of parameters	Prior distribution	Other constraints
Spatially aggregated average recruitment	$\bar{R}$	1	Uninformative	
Stock-recruitment parameter (spatially aggregated)	β'	1	Uninformative	
Spatially aggregated recruitment deviations	φ_t	151	Weak, mean of 0	Weak smoothing penalty, $\sum_t \varphi_t = 0$, very weak penalty on deviation from stock-recruitment relationship
Average spatial distribution of recruitment	α_r	6	Uninformative	$\sum_r \alpha_r = 1$
Recruitment spatial distribution deviations	γ_{tr}	906	Weak, mean of 1	$\prod_t \gamma_{tr} = 1$, $\sum_r \alpha_r \gamma_{tr} = 1$
Age-dependent natural mortality	M_a	20	Uninformative	Moderate smoothing penalty across age
Movement parameters	ϕ_0^{xy}, ϕ_1^{xy}	36	Weak, mean of 0	
Selectivity	s_{af_r}	187	Uninformative	Range 0–1, increasing function of age for LL1–LL7, moderate smoothing penalty across age
Catchability in year 1	q'_{1f_r}	10	Uninformative	
Catchability deviations	η_{yf_r}	71	Various (see text)	
Seasonal catchability	c_{1f_r}, c_{2f_r}	26	Weak, mean of 0 (fish. 4–16)	
Effort deviations	ε_{tf_r}	1941	Moderate, mean of 0	
Mean lengths-at-age for age classes 2–8	μ_a	7	Uninformative	Increasing with age
von Bertalanffy growth parameters	L_1, L_A	3	Uninformative	
Variance of length-at-age	λ_1, λ_2	2	Uninformative	
Tag-reporting rates	X_{f_r}	16	See Table D1	Range 0–1
Negative binomial parameters	$\varpi_{f'_r}$	13		
Total		3397		